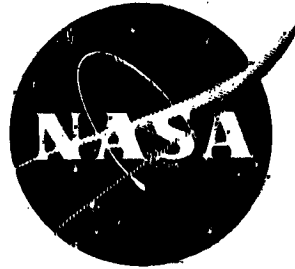


NASA CR-134546

BCAC D6-43089



CRUISE DRAG RESULTS FROM HIGH-SPEED WIND TUNNEL TESTS
OF NASA REPAI JT8D ENGINE NACELLES

ON THE BOEING 727-200

(NASA-CR-134546) CRUISE DRAG RESULTS
FROM HIGH-SPEED WIND TUNNEL TESTS OF
NASA REPAI JT8D ENGINE NACELLES ON THE
BOEING 727-200 (BOEING CO., CHICAGO,
WASH.) 9. 1. 63. 25 CSCL 01C 63/02 29039
N74-18673
Unclass

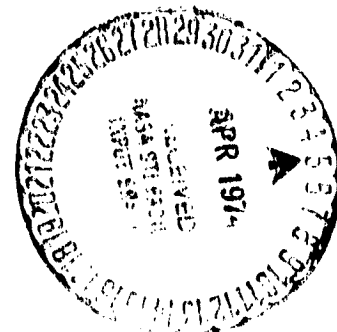
by W. G. Easterbrook and R. B. Carlson

BOEING COMMERCIAL AIRPLANE COMPANY
A DIVISION OF
THE BOEING COMPANY

Prepared for
NATIONAL AERONAUTICS AND SPACE ADMINISTRATION

NASA Lewis Research Center

Contract NAS3-17842



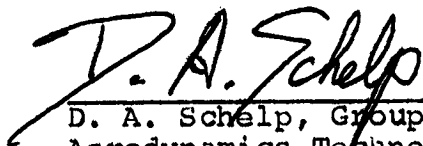
1. Report No. NASA-CR-134546		2. Government Accession No.		3. Recipient's Catalog No.	
4. Title and Subtitle Cruise Drag Results From High Speed Wind Tunnel Tests of NASA Refan JT8D Engine Nacelles on the Boeing 727-200				5. Report Date December 1973	
				6. Performing Organization Code	
7. Author(s) W. G. Easterbrook and R. B. Carlson				8. Performing Organization Report No. DG-43099	
9. Performing Organization Name and Address The Boeing Company Seattle, Washington 98124				10. Work Unit No.	
				11. Contract or Grant No. NAS 3-17842	
12. Sponsoring Agency Name and Address National Aeronautics and Space Administration Washington, D. C. 20546				13. Type of Report and Period Covered Contractor Report	
				14. Sponsoring Agency Code	
15. Supplementary Notes Project Manager, A. A. Medeiros NASA/Lewis Research Center, Cleveland, Ohio 44135					
16. Abstract High speed wind tunnel test results are presented showing the cruise drag effect of installing JT8D-109 Refan engines on a Boeing 727-200. Incremental drags of a Refan center inlet and side nacelles are presented for several configuration variations. Static pressure distributions were obtained on the side nacelle strut and on the fuselage (above and below the strut). Oil flow photographs of selected configurations are also presented. In general the drag level of the refan installation is slightly better than predicted prior to the test and the drag rise is favorable.					
17. Key Words (Suggested by Author(s)) 727-200 Refanned JT8D Engine Cruise Drag High Speed Wind Tunnel Test				18. Distribution Statement	
19. Security Classif. (of this report) Unclassified		20. Security Classif. (of this page) Unclassified		21. No. of Pages 42	
				22. Price*	

* For sale by the National Technical Information Service, Springfield, Virginia 22151

FOREWORD

The high-speed wind tunnel tests described in this report were performed by the Aerodynamics Technology Staff of the Boeing Commercial Aiplane Company, a division of The Boeing Company, Seattle, Washington. The work, sponsored by NASA Lewis Research Center and reported herein, was performed between August and November 1973.

This report has been reviewed and is approved by:



D. A. Schelp, Group Engineer
Aerodynamics Technology Staff

FEB 12, 1974

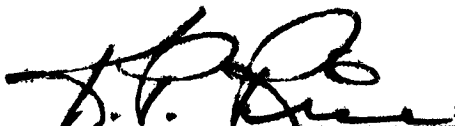
Date



J. A. Ferrell, Chief, Technology Staff
JT8D Refan Program

FEB 18, 1974

Date



K. P. Rice, Program Manager
JT8D Refan Program

2/19/74

Date

PRECEDING PAGE BLANK NOT FILMED

TABLE OF CONTENTS

	<u>Page</u>
1.0 SUMMARY -----	1
2.0 INTRODUCTION -----	3
3.0 NOMENCLATURE -----	5
4.0 MODEL AND TEST DESCRIPTION -----	7
4.1 MODEL -----	7
4.2 TEST FACILITY AND MODEL INSTALLATION -----	7
4.2.1 CALSPAN TRANSONIC WIND TUNNEL -----	8
4.2.2 BOEING TRANSONIC WIND TUNNEL -----	8
5.0 TEST RESULTS AND DISCUSSION -----	9
6.0 CONCLUSIONS -----	15
7.0 FIGURES -----	17

PRECEDING PAGE BLANK NOT FILMED

1.0 SUMMARY

Two high speed wind tunnel tests were conducted to investigate the effect of JT8D-109 refan nacelles on Boeing 727-200 cruise drag. The first test was aimed at determining the side nacelle and center inlet contours. The second test was conducted to complete the investigation of fairings at the fuselage-nacelle strut intersection and nacelle strut chord extensions. These fairings and nacelle strut modifications were designed to alleviate a local flow separation at the aft end of the nacelle strut-fuselage intersection. The following conclusions about the nacelle and center inlet configurations were reached from the test results:

- The drag level penalty for refan nacelles is less than the predicted value.
- Drag rise of the refan installation is better than that of the production nacelle installation.
- The side nacelle contour is acceptable with a straight sided portion (cylindrical) near the center to facilitate interchangeability of right and left nacelle cowl doors.
- No inboard canting of the inlet highlight plane is required for the side nacelles. This permits interchangeability of right and left inlets. (Production 727-200 has 4° inboard cant.)

- The side nacelle strut configuration should include an aft strut-fuselage fairing or aft strut chord extension.
- Center engine inlet contours were satisfactory as initially defined for the refan engine.

2.0 INTRODUCTION

The Pratt & Whitney Aircraft JT8D-109 engine is a derivative of the basic JT8D-9 turbofan engine, modified to incorporate a new, larger diameter, single-stage fan with a bypass ratio of 2.03 and two supercharging low-pressure compressor stages. The modification gives lower jet noise, increased takeoff and cruise thrust, and lower specific fuel consumption. The use of the JT8D-109 engine on the Boeing 727 airplane will require enlarged side engine nacelles and center engine inlet. The affected regions on the airplane are indicated on the airplane general arrangement shown on Figure 1. The effects of these larger nacelles and center inlet on the low speed stability and control characteristics of the 727-200 were investigated in the Boeing Vertol Wind Tunnel during May and June 1973. The results of these low speed tests are reported in NASA CR-134503. This investigation largely determined the positioning of the nacelles relative to the fuselage.

Two high speed wind tunnel tests were then run to determine the Boeing 727-200 NASA Refan Nacelle external contours and to provide the basis for prediction of the resultant incremental cruise drag. The first test was conducted in the CALSPAN Transonic Wind Tunnel in Sept. 1973. The principal purpose of this first high speed test was to investigate the effects of side nacelle contour changes. A second high speed test was

conducted in the Boeing Transonic Wind Tunnel, in Oct. 1973, to further investigate the nacelle strut configuration. The pertinent test results from those two high speed tests are analyzed and presented in this report. The results from these tests were used in determining the NASA Refan external configuration and to predict the associated incremental cruise drag of the selected configuration.

3.0 NOMENCLATURE

C_L	Airplane lift coefficient, lift/ $q_\infty S$
C_D	Airplane drag coefficient, drag/ $q_\infty S$
ΔC_D (Net)	C_D with Refan side nacelles and center duct minus C_D with production side nacelles and center duct.
ΔC_D (Center Inlet)	C_D with center inlet minus C_D with no center inlet
ΔC_D (Nacelle)	C_D with side nacelles minus C_D with no side nacelles
ΔC_D (Improv.)	C_D without fairing or extended strut chord minus C_D with fairing or extended strut chord.
C_p	Pressure coefficient, $\frac{P_L - P_\infty}{q_\infty}$
M	Mach No.
α	Wing angle of attack
Re/Ft	Reynolds number per foot, $\frac{\rho_\infty V_\infty}{\mu_\infty}$
CALSPAN	CALSPAN Corporation Transonic Wind Tunnel
BTWT	Boeing Transonic Wind Tunnel
P_L	Local static pressure psf
P_∞	Freestream static pressure psf
q_∞	Freestream dynamic pressure, $0.7P_\infty M^2$, psf
V_∞	Freestream velocity ft/sec.
μ_∞	Freestream viscosity
ρ_∞	Freestream static density
S	Wing reference area ft ²

4.0 MODEL AND TEST DESCRIPTION

4.1 MODEL

An existing .046 scale model of the 727-200 airplane was used. Production and Refan center ducts and nacelles were flow through type. Side nacelle construction consisted of an aluminum body with epoxy contours (inlet lips were solid aluminum contours with no epoxy covering). The center engine duct was made of a molded fiberglass duct from a solid aluminum inlet lip and exit piece. Inlet velocity ratios appropriate to cruise thrust were obtained with the side nacelles and center duct by slightly opening up the exit area of the nacelle. The fuselage was built with a steel inner body structure, aluminum bulkheads and fiberglass skins. The wing consisted of a steel spar with epoxy contours. The wing was made up of right and left panels connected by an incidence block.

4.2 TEST FACILITIES AND MODEL INSTALLATIONS

Tests in CALSPAN and BTWT transonic tunnels were run at nearly the same Reynolds numbers. Corrections were made to C_D values for variances from a nominal Reynolds number schedule with Mach number. The C_D correction was based on the variation of flat plate turbulent skin friction with Reynolds number. The following nominal Reynolds numbers were used:

PRECEDING PAGE BLANK NOT FILMED

Re/ft. $\times 10^{-6}$		
<u>Mach No.</u>	<u>(Calspan)</u>	<u>(BTWT)</u>
.70	3.375	3.33
.78	3.595	3.51
.80	3.65	3.55
.82	3.705	3.588
.84	3.76	3.626
.86	3.815	3.662
.88	3.87	3.696

4.2.1 CALSPAN Transonic Wind Tunnel

The model was plate mounted with an island fairing around the base of the plate (Fig. 2). A strain gage force balance was used for measuring model forces on the plate.

4.2.2 Boeing Transonic Wind Tunnel

The model was similarly plate mounted on an island fairing (Fig. 3) but this time the tunnel main external force balance was used for force measurements.

5.0 TEST RESULTS AND DISCUSSION

Data acquired during the two high speed wind tunnel tests included model force measurements, static pressure measurements, and flow visualization with fluorescent oil. Internal drag of the flow nacelles and center duct were calculated using an existing boundary layer computer program. Velocity distributions were calculated using static pressure measurement inside the nacelles near the exit to establish actual internal flows. Internal drag values are subtracted from nacelle drag increments in all cases. All surfaces were tripped with strips of distributed grit. Test configurations are pictured on Fig. 4 to 6. A summary sketch showing refan nacelle configurations is presented on Fig. 7.

The first test was intended to provide the basis for establishing side nacelle and center inlet configurations. Also, some initial work was done to define a strut/fuselage aerodynamic fairing or strut chord extension to remedy a local flow separation discovered at the intersection of strut and fuselage (aft end). This work was continued during the second test and a suitable fairing or lengthened strut was developed. The overall net drag increment due to the refan nacelle configuration is given on Fig. 8. This includes the improvement gained by a strut/fuselage fairing.

Specific drag effects are presented on the next figures. The first comparison is between standard and refan center inlets on Fig. 9. Little difference resulted. The two configurations differ principally in inlet diameter, inlet lip height above the fuselage, and the angle of the highlight plane. Comparisons of some principal dimensions are given below:

<u>Center Inlet</u>	<u>Highlight Dia.</u>	<u>Lip Height Above Fuselage</u>	<u>Angle of Inlet Axis to Fuselage</u>
Production	43.7 in.	15.8 in.	0°
Refan	54.5 in.	17.0 in.	3°40'

Drag increments for standard and refan nacelles are given in Fig. 10. Corresponding oil flow photos are shown on Figs. 11 and 12. The refan configuration has a drag level increase but more favorable drag rise characteristics as compared to the production airplane. Principal dimensions of the configurations are indicated below:

<u>Nacelle</u>	<u>Highlight Dia.</u>	<u>Maximum Dia.</u>	<u>Length</u>
Production	42.0 in.	50.0 in.	217.1 in.
Refan	52.2 in.	62.0 in.	233.1 in.

A check of trip effect was made on the refan nacelle by removing external grit strips. No discernable change resulted.

The effect on drag of canting the side nacelle inlet highlight plane inboard by 3° (relative to the nacelle axis) is shown on Fig. 13. The standard production nacelle has a highlight cant of 4° inboard. It appears that drag level with the 3° cant is higher and the drag rise slightly worse. Thus, the advantage of permitting common right and left hand inlet installations on the airplane can be obtained.

Another effect studied was that of side nacelle contour. Two contour alternatives were proposed:

- A contour with a straight-sided (cylindrical) portion in the middle to facilitate the design and manufacture of cowl doors. With a cylindrical portion, cowl doors can be made to be common on right and left hand engine installations.
- A fully contoured shape with a continuous curvature distribution from front to rear. This would normally provide the best aerodynamic design for a nacelle.

Drag results are shown on Fig. 14 with the straight sided version having an unexpected lower drag level. Local flow effects appear to predominate over expected isolated nacelle drag results. The maximum diameter of the fully contoured shape occurs near where peak pressures are indicated on the strut. This aggravates

the local velocity distribution on the inboard portion of the nacelle and worsens drag.

A local flow separation was discovered at the aft end of the intersection between the side nacelle strut and fuselage. The oil flow photo on Fig. 12 shows this on the bottom view of the strut. Six nacelle strut-body intersection fairings and two nacelle strut chord extensions were tested in an effort to curb this problem. Figs. 15 and 16 show the drag improvements for the most favorable fairing and strut chord extension as determined by size and drag improvement. Corresponding oil flow photos with the modifications are presented on Fig. 17 and 18. The separation is remedied in both cases with a resultant drag improvement. The net refan drag previously shown on Fig. 8 included the benefit from the nacelle strut fairing.

Static pressures were measured in the vicinity of the side nacelle.

- Two rows of pressure ports on the fuselage - one above and one below the nacelle strut.
- Two rows of ports on the strut - one on the upper and one on the lower surface.

A sketch of these locations relative to the nacelle is shown on Fig. 19. Various static pressure comparisons are given on Figures 20 thru 24 to show effects of nacelle, Mach No., etc.

Several interesting effects can be seen. The general level of C_p from body alone data indicates a significant high velocity distribution in the nacelle area because of the boattail effect of the body closure. There is a significant shock evident on the strut at .84 Mach number (Fig. 21) with the nacelle installed. The increased supersonic velocity of the strut added to the negative C_p due to the body closure causes a shock just aft of the strut leading edge. These effects are evident for both the production and refan configurations. Fig. 20 indicates little difference in pressure distributions between Refan and Production configurations. A strut leading edge modification was tried in an attempt to weaken the shock but demonstrated no drag benefit. The flow problem is such that an extensive change to the configuration would be required to eliminate the shock (fuselage dishing, moving nacelle etc.). These fixes were considered beyond the scope of the Refan Program.

6.0 CONCLUSIONS

Analysis of data from two 727 refan tests has permitted the following conclusions to be made concerning the refan nacelle configurations:

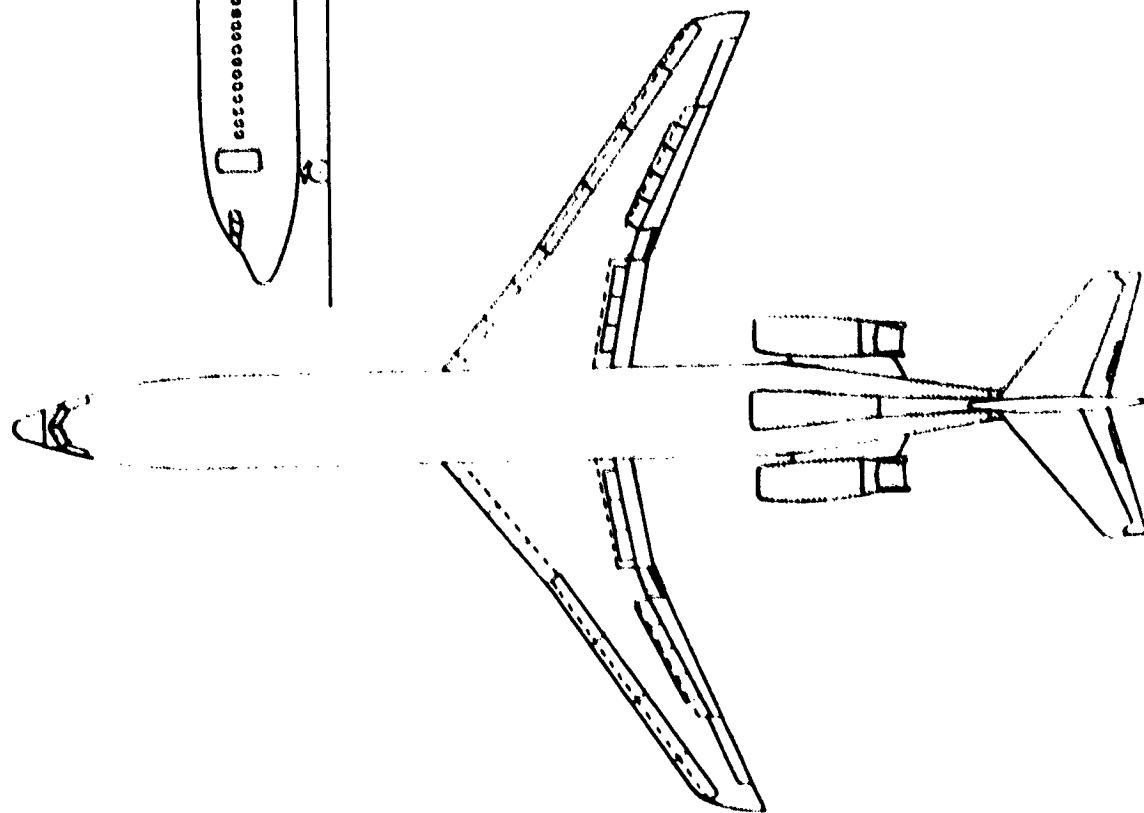
- A refan side nacelle with a straight sided (cylindrical) portion has lower drag than a nacelle having a fully contoured shape (continuous curvature variation).
- Canting the highlight plane of the inlet inboard by 3° for side nacelles was found to be unnecessary. Drag measurements with and without the 3° cant showed no improvement with 3° of inlet cant. Thus, a straight inlet could be designed to be common for right and left hand nacelle installations.
- Static pressure measurements were made on the fuselage, above and below the nacelle and on upper and lower strut surfaces. These pressures indicate the existence of a shock between the fuselage and nacelle just aft of the strut leading edge. The shock occurs both on the basic 727 and refan nacelle configurations.
- The drag penalty due to refan nacelles is lower than that estimated prior to the test so the nacelle configuration appears satisfactory.

- A strut/fuselage fairing at the aft end of the side nacelle strut or an aft strut chord extension provides a drag improvement.

7.0 LIST OF FIGURES

<u>Figure</u>	<u>Title</u>	<u>Page</u>
1	727-200/JT8D-109 Refan Airplane	19
2	727-200 Model Installation in Calspan Wind Tunnel	20
3	727-200 Model Installation in BTWT Wind Tunnel	21
4	Production and Refan Nacelle Configurations	22
5	Refan Nacelle Configuration on Model	23
6	Refan Strut/Fuselage Fairing and Strut Chord Extension	24
7	Sketches of Refan Nacelle Model Configurations	25
8	Net Drag Increment Due to Refan Installation	26
9	Drag of Production and Refan Center Inlets	27.
10	Drag of Production and Refan Side Nacelles	28
11	Oil Flow - Production Nacelle	29
12	Oil Flow - Refan Straight-Sided Nacelle	30
13	Drag Effect of Canting Highlight Plane of Side Nacelle	31
14	Drag Effect of Side Nacelle Contour Variation	32
15	Drag Improvement of Strut/Fuselage Fairing	33
16	Drag Improvement of Strut Chord Extension	34
17	Oil Flow - Refan Strut/Fuselage Fairing	35
18	Oil Flow - Extended Chord Strut	36
19	Sketch of Fuselage and Nacelle Strut Pressure Port Locations	37
20	Comparison of Production and Refan Static Pressures	38
21	Static Pressures With and Without Refan Side Nacelle (Upper Fuselage and Strut)	39

<u>Figure</u>	<u>Title</u>	
22	Static Pressures With and Without Refan Side Nacelle (Lower Fuselage and Strut)	40
23	Effect of Mach No. on Refan Static Pressures (Upper Fuselage and Strut)	41
24	Effect of Mach No. on Refan Static Pressures (Lower Fuselage and Strut)	42



AREAS AFFECTED
BY REPAIR ENGINE
INSTALLATION

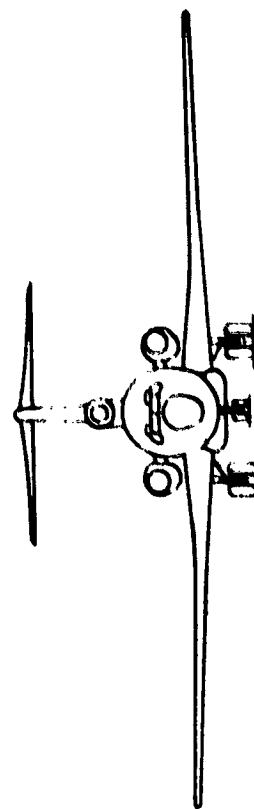


FIGURE 1 - 727-200 JT8D-109 PEFAN AIRPLANE

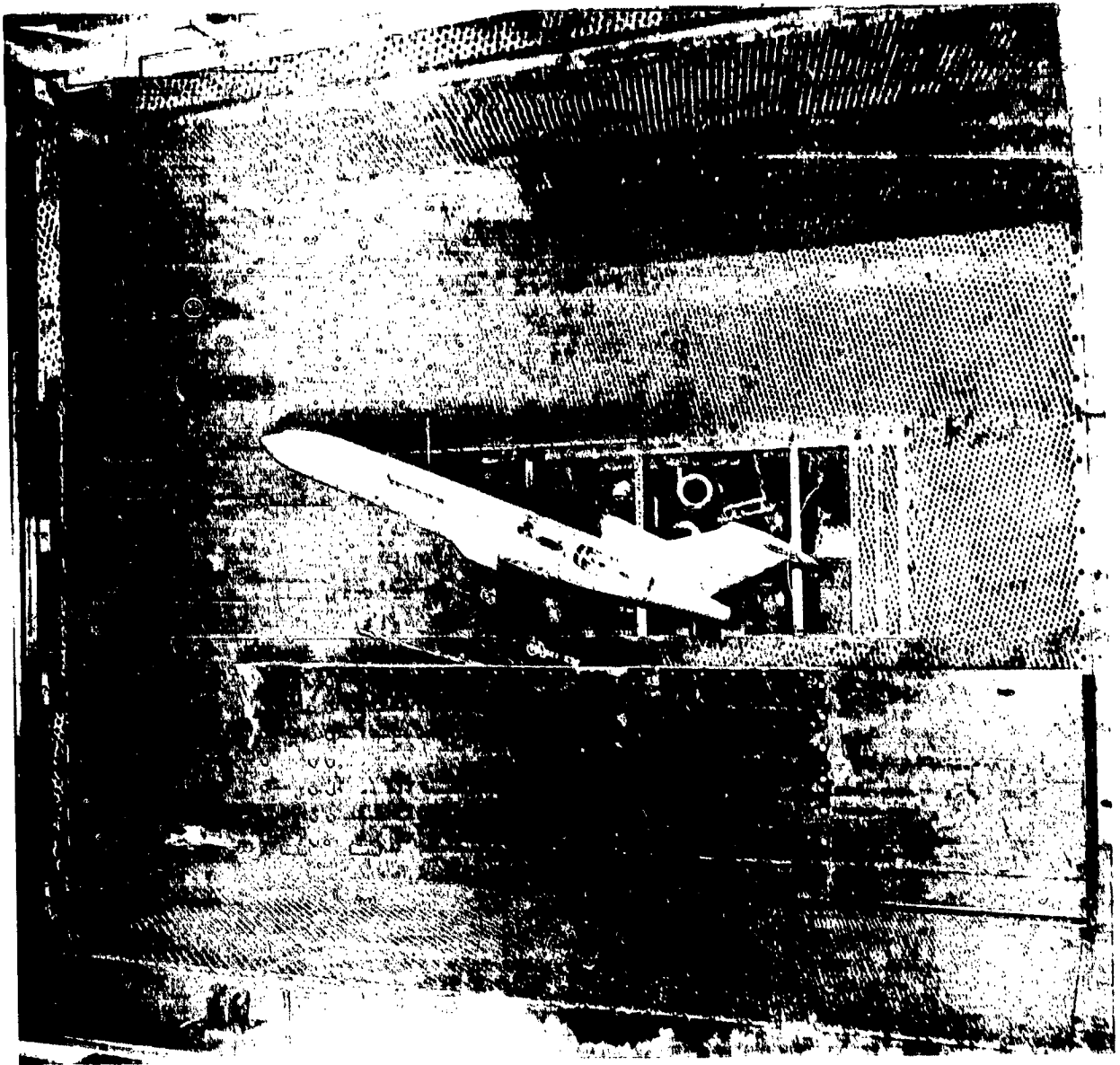


FIGURE 2 227 200 MODEL INSTALLATION IN CALSPAN WIND TUNNEL



FIGURE 3 727-200 MODEL INSTALLATION IN BTWT WIND TUNNEL

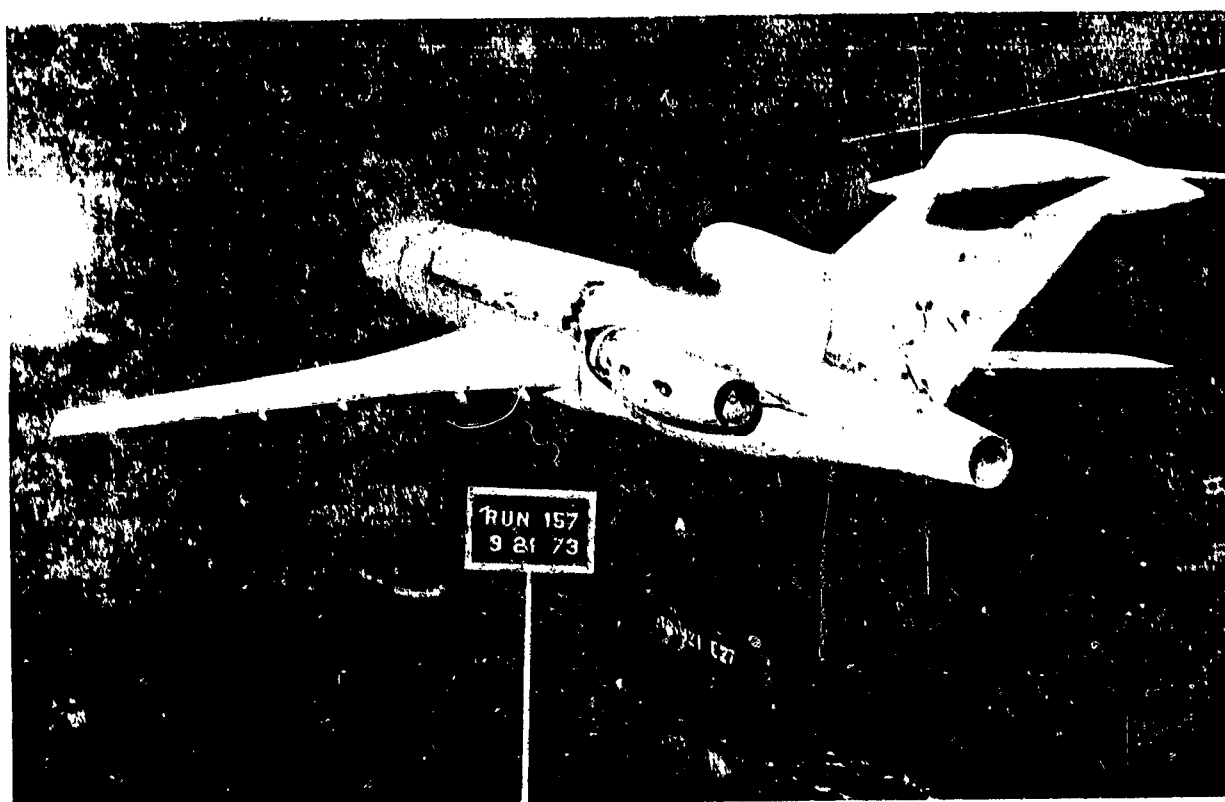
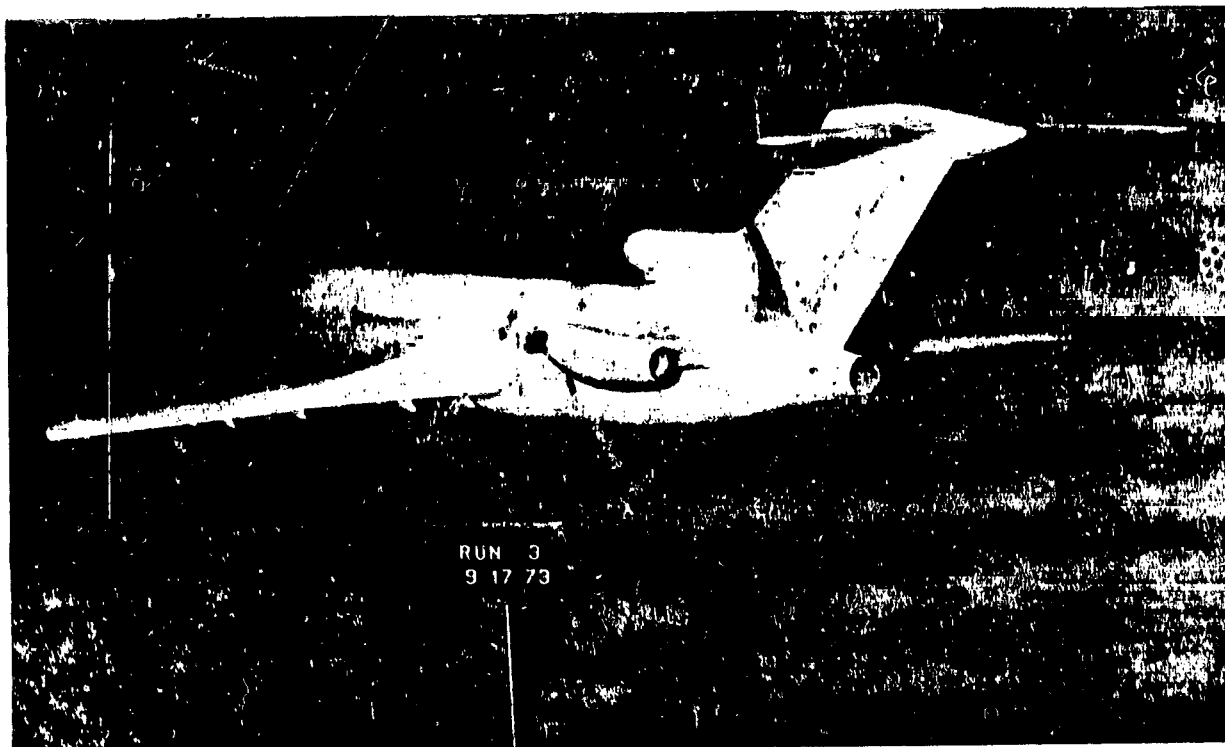


FIGURE 4 PRODUCTION AND REFAN NACELLE CONFIGURATIONS

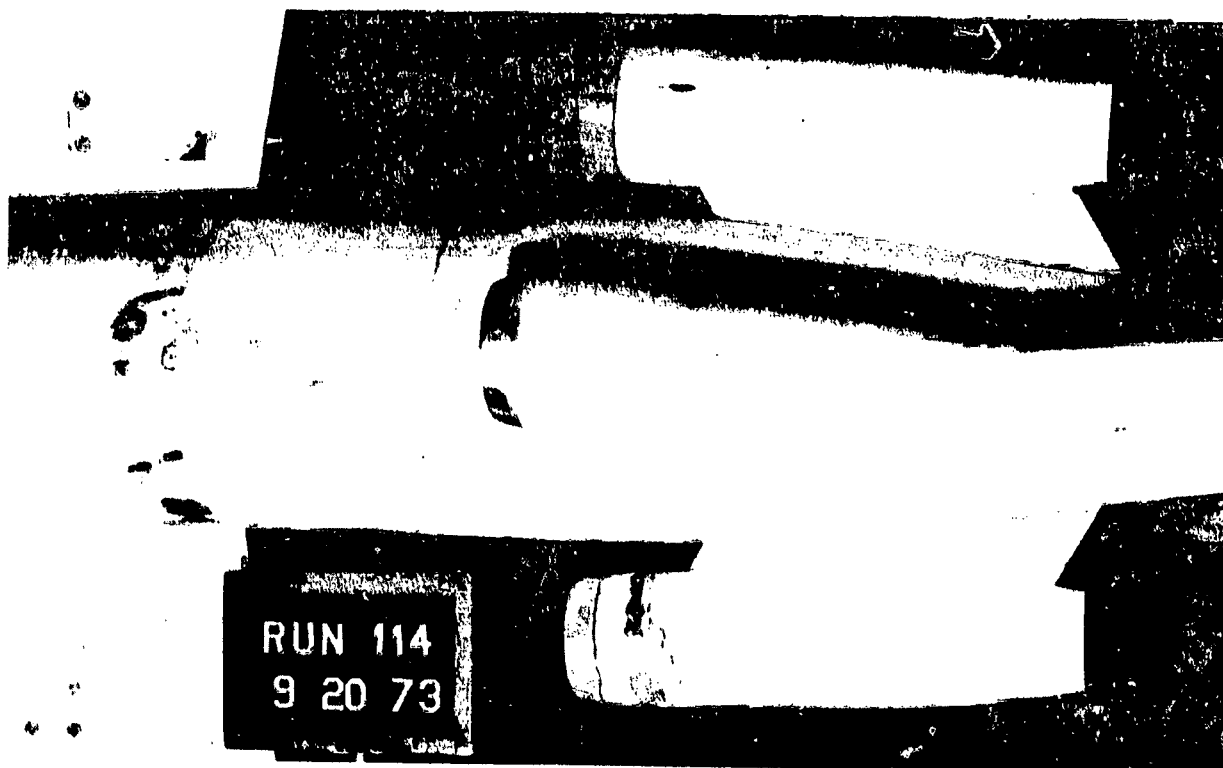
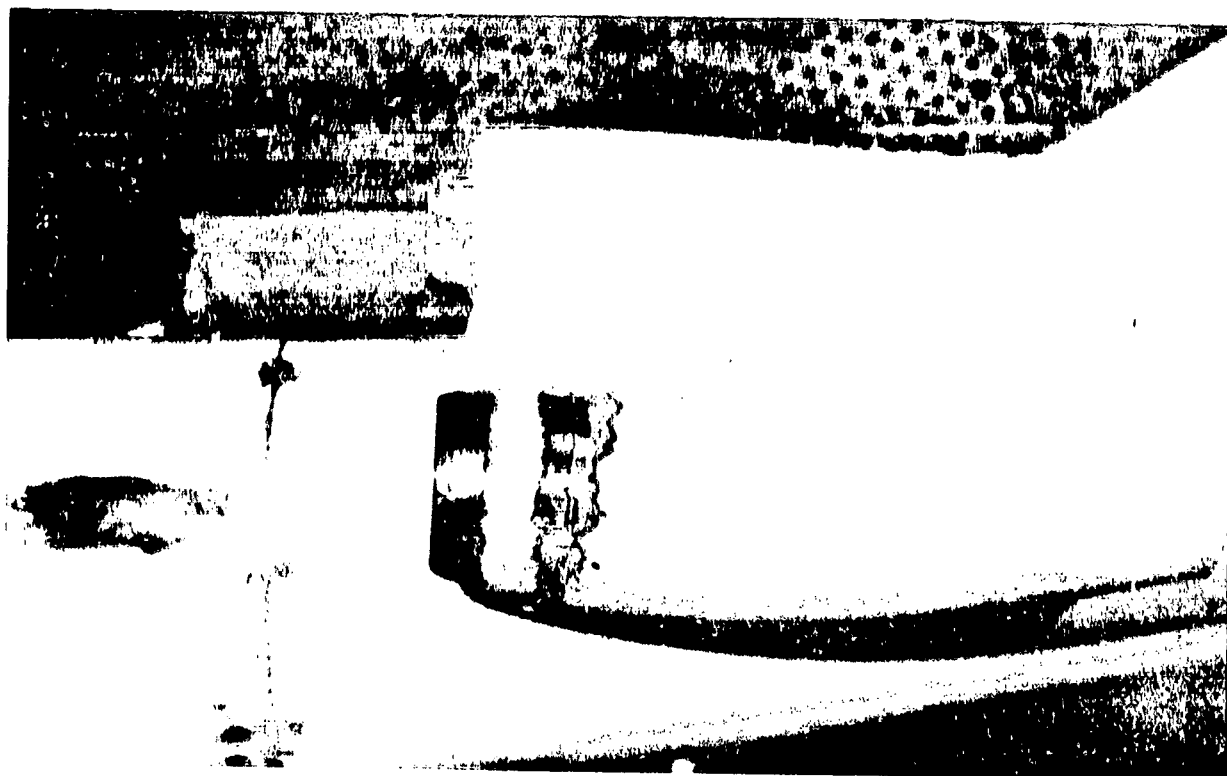


FIGURE 5 REFAN NACELLE CONFIGURATION ON MODEL

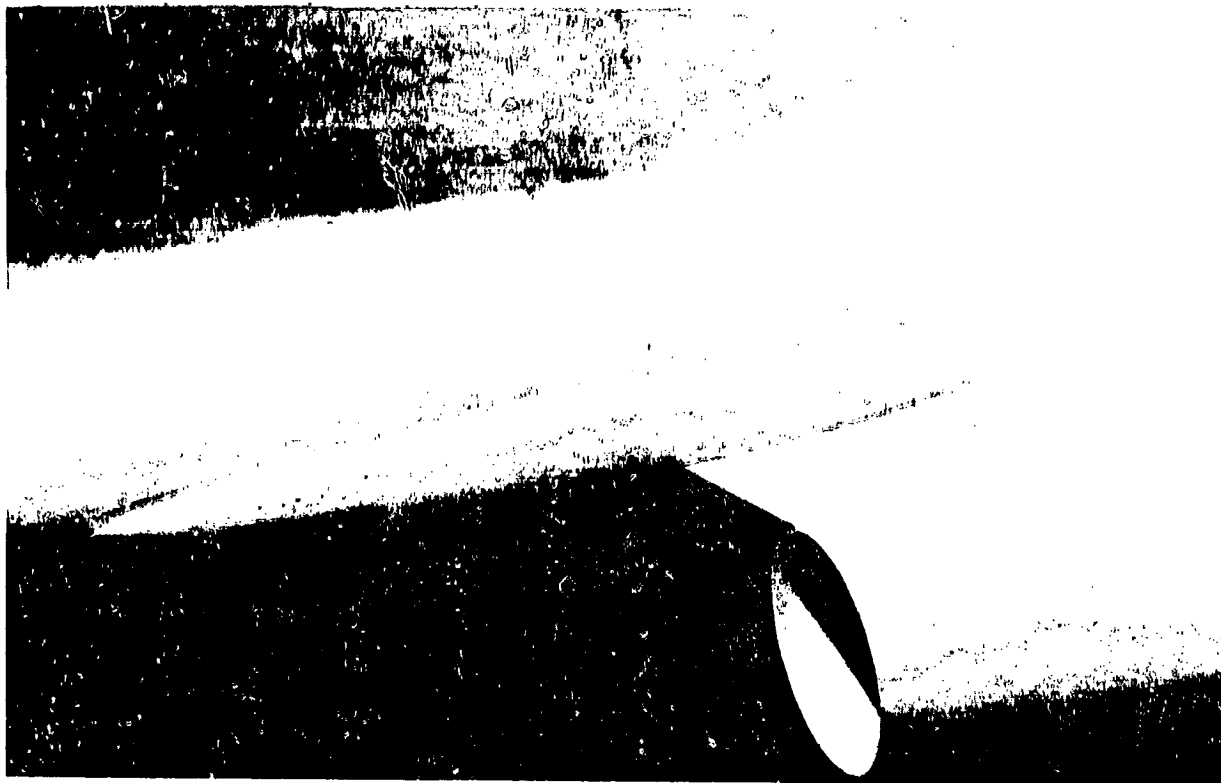


FIGURE 6 REFAN STRUT/FUSELAGE FAIRINGS AND STRUT CHORD EXTENSION

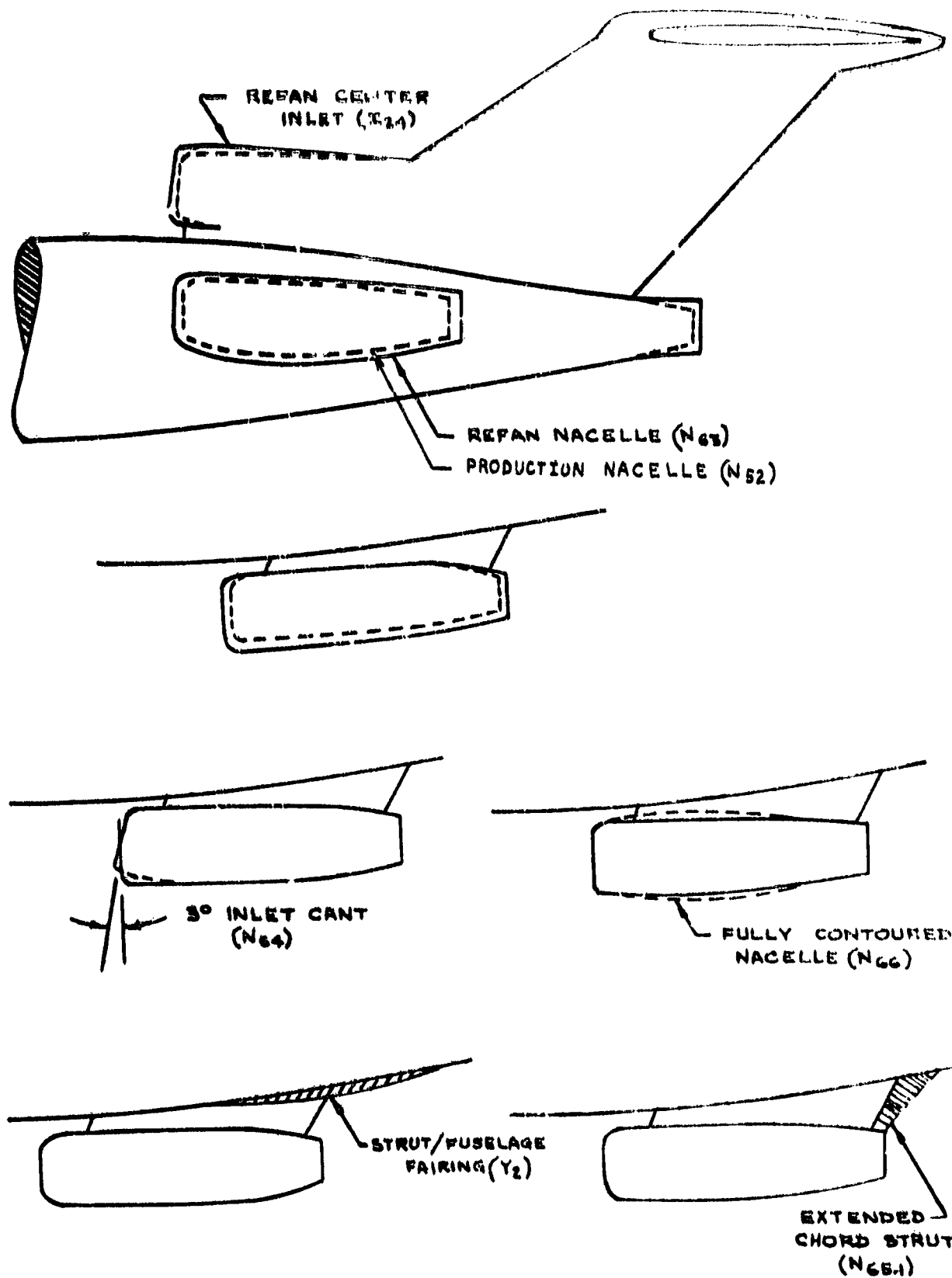


FIGURE 7 SKETCHES OF REFAN NACELLE MODEL CONFIGURATIONS

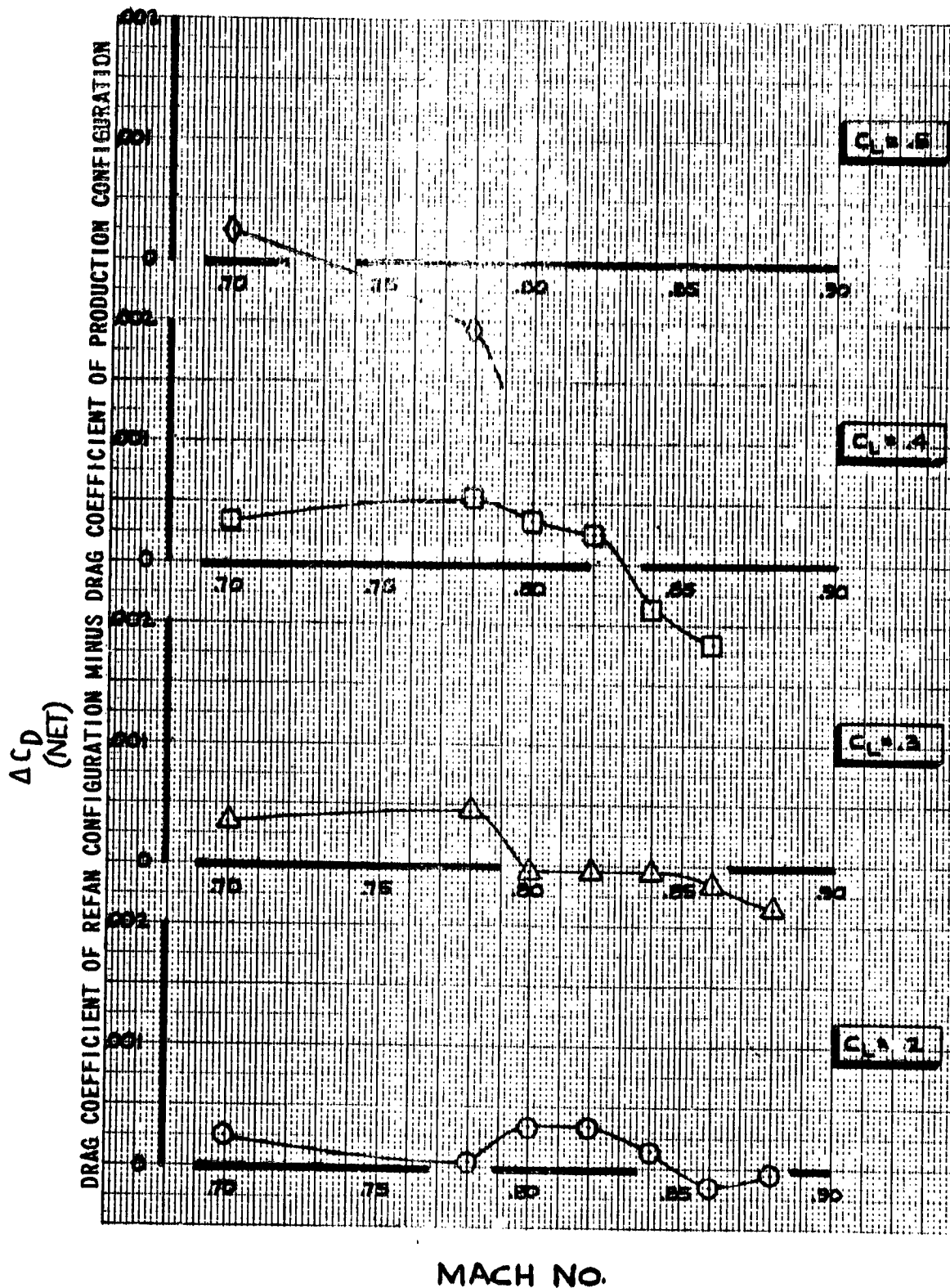


FIGURE 8 NET DRAG INCREMENT DUE TO REFAN INSTALLATION

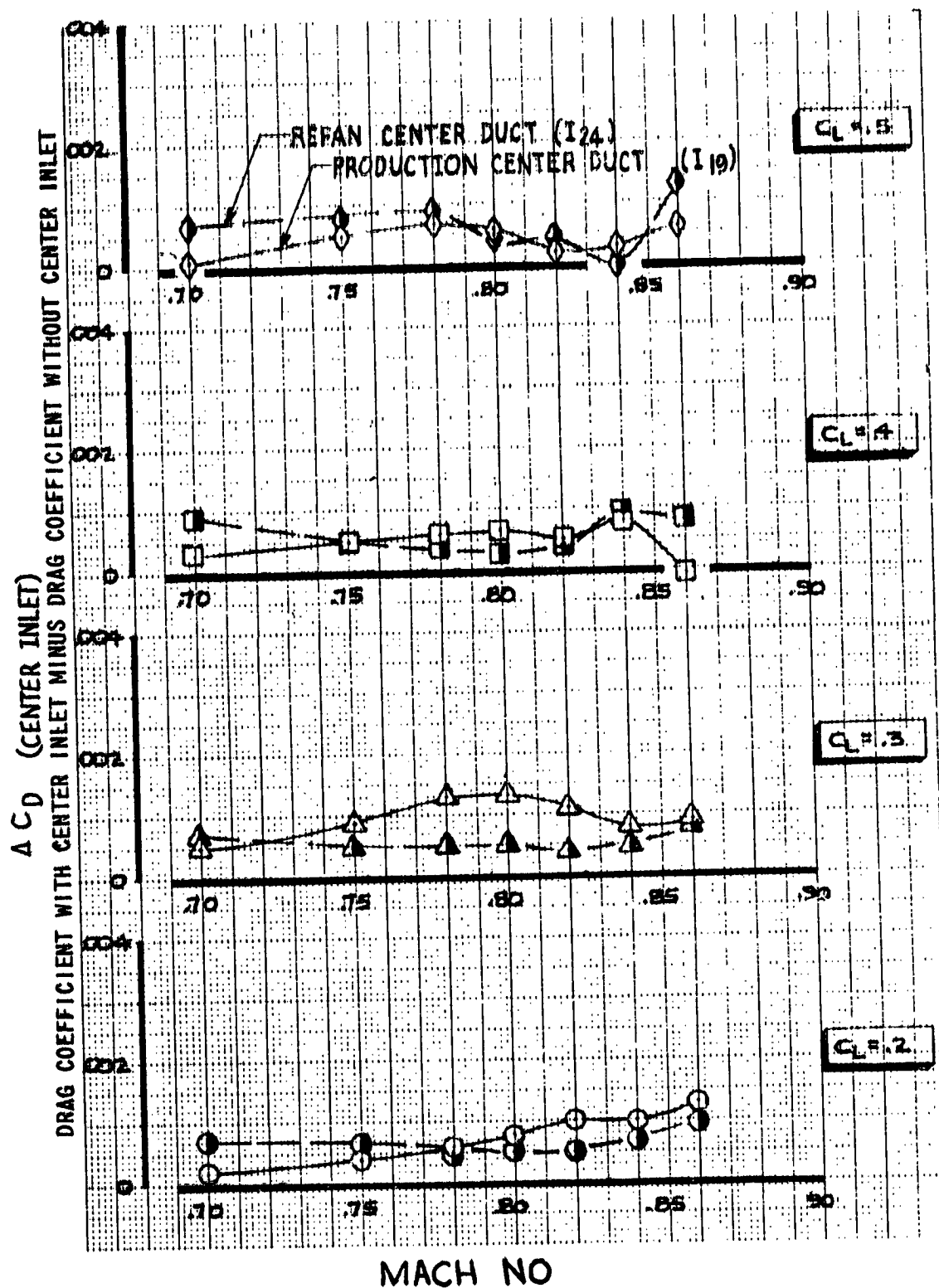


FIGURE 9 DRAG OF PRODUCTION AND REFAN CENTER INLETS

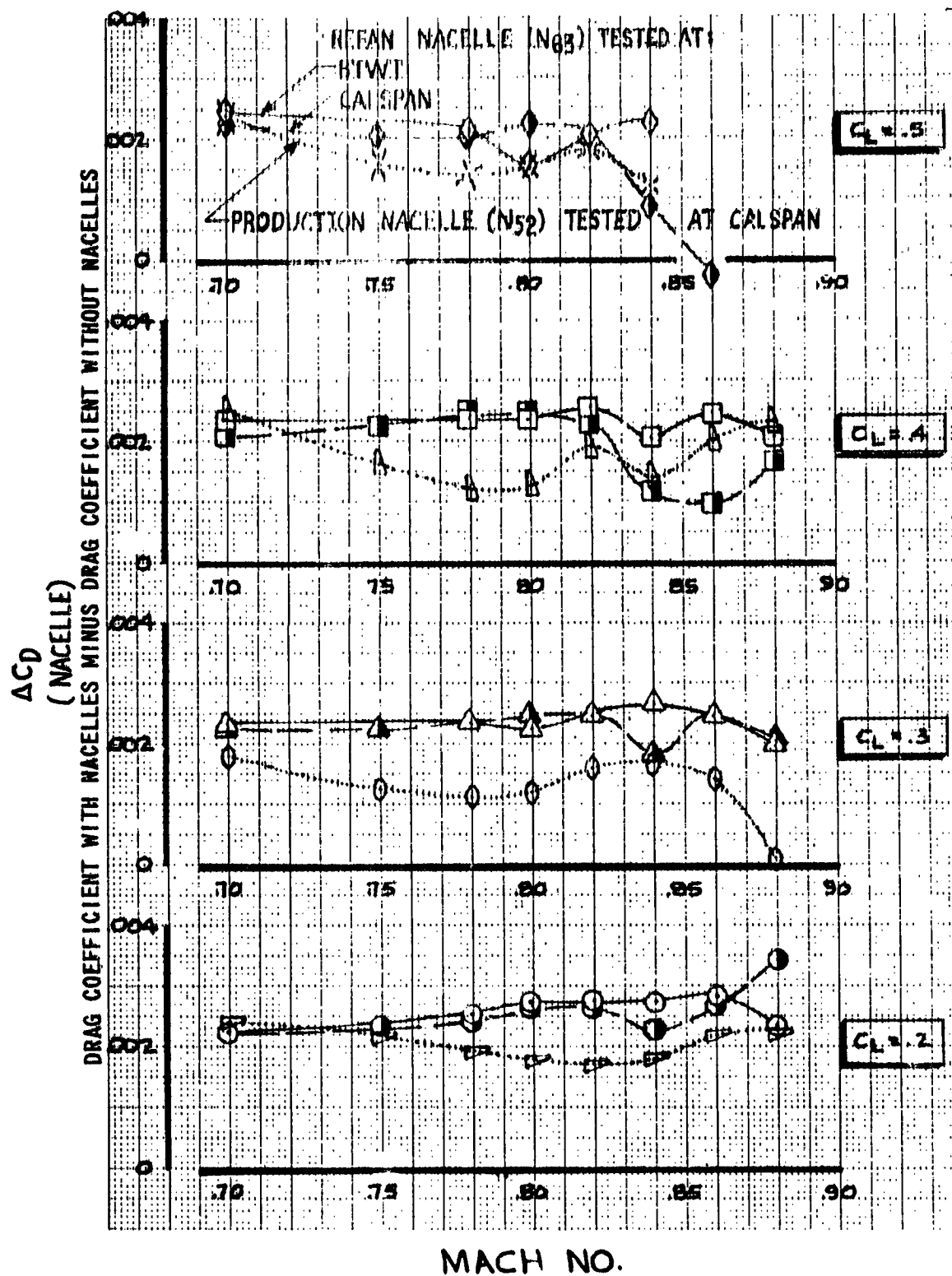


FIGURE 10 DRAG OF PRODUCTION AND REFAN SIDE NACELLES

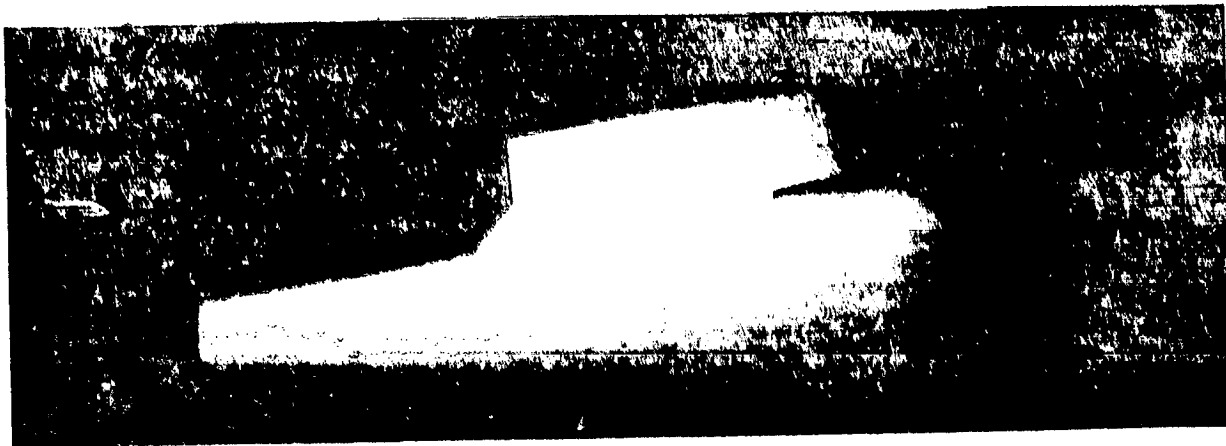
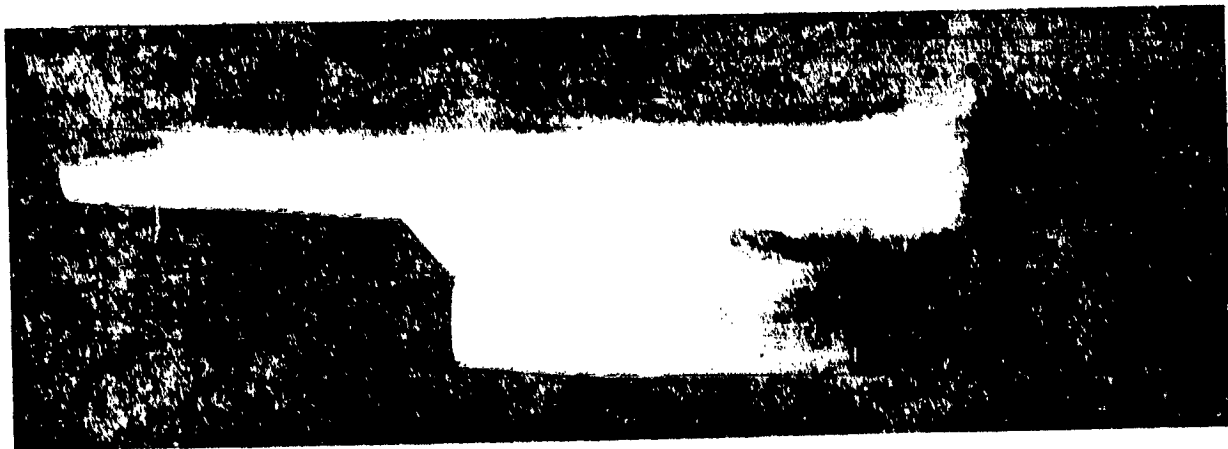


FIGURE 11 OIL FLOW - PRODUCTION NACELLE

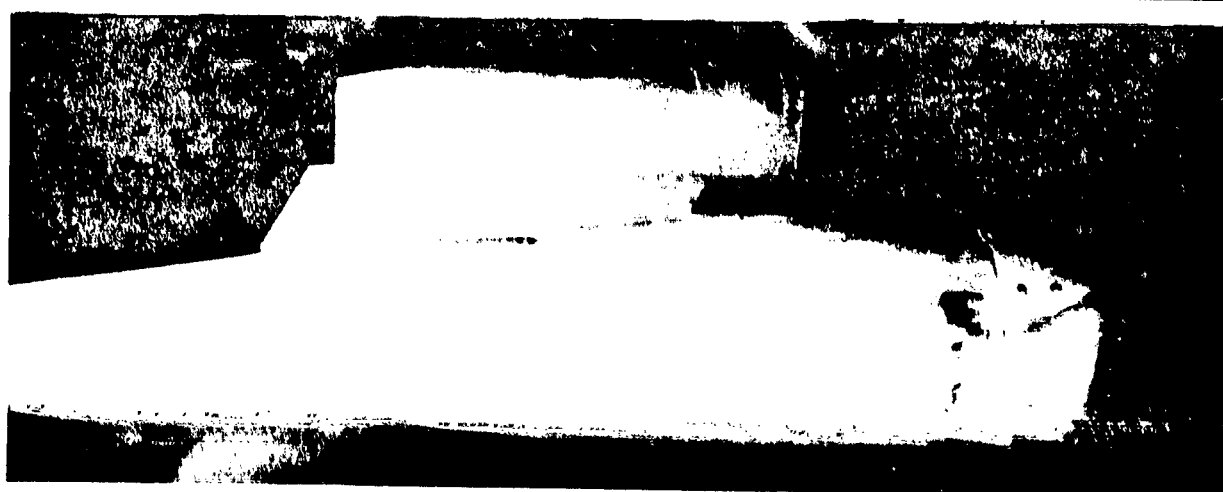
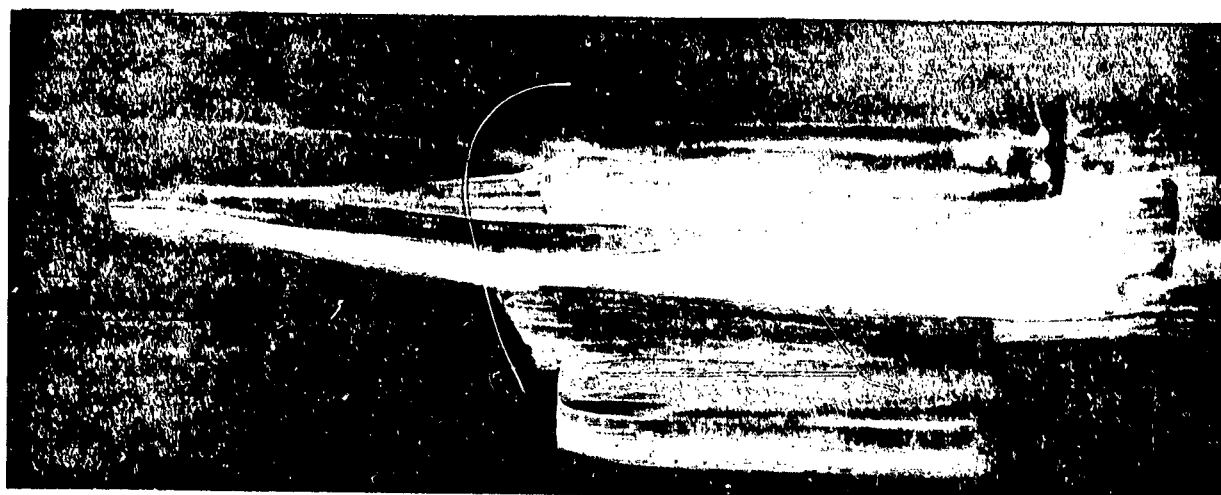
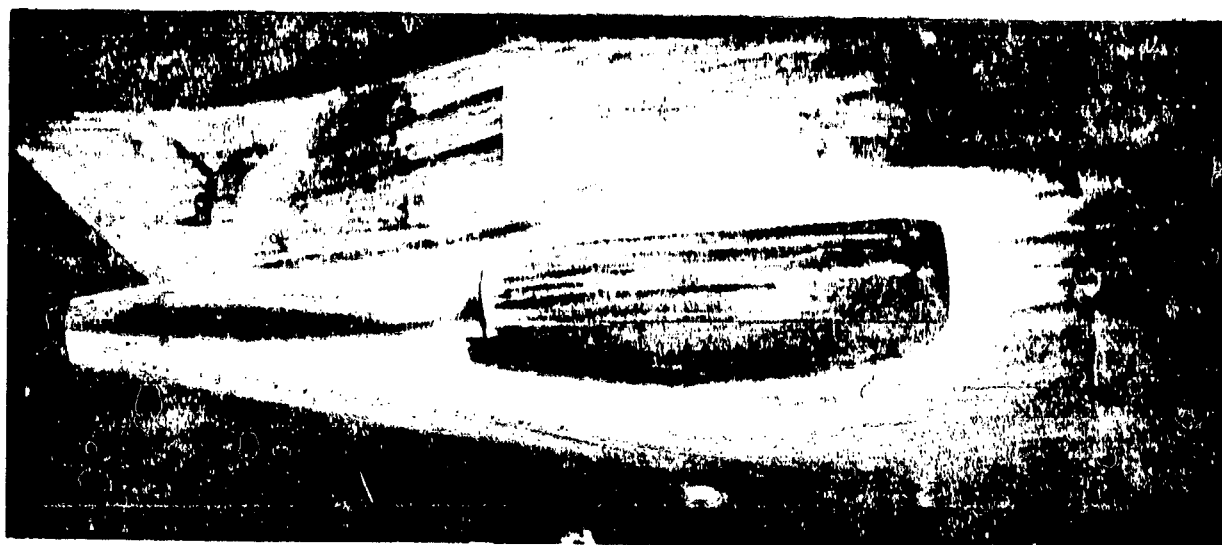


FIGURE 12 OIL FLOW - REFAN STRAIGHT SIDED NACELLE

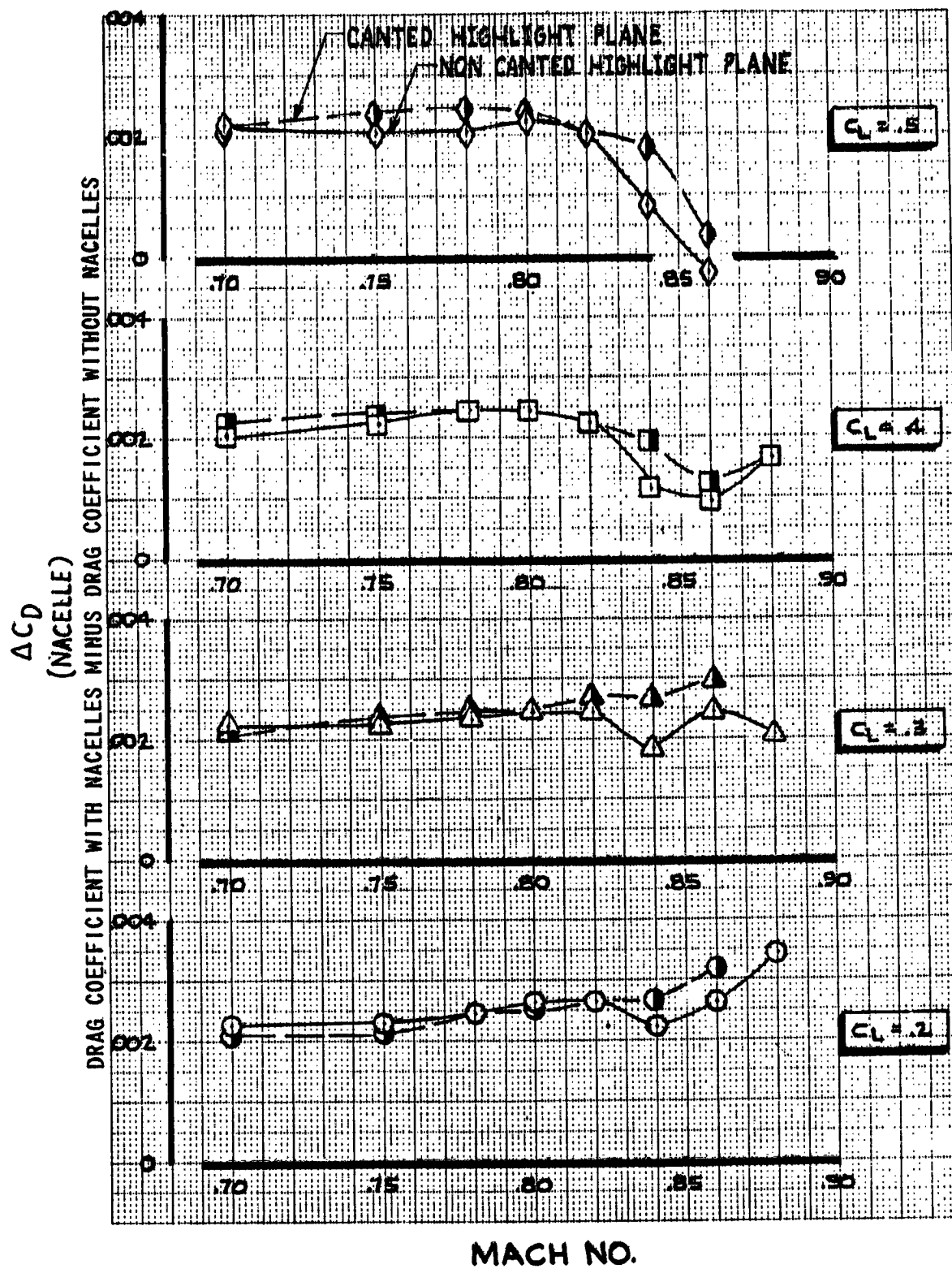


FIGURE 13 DRAG EFFECT OF CANTING HIGHLIGHT PLANE OF SIDE NACELLE

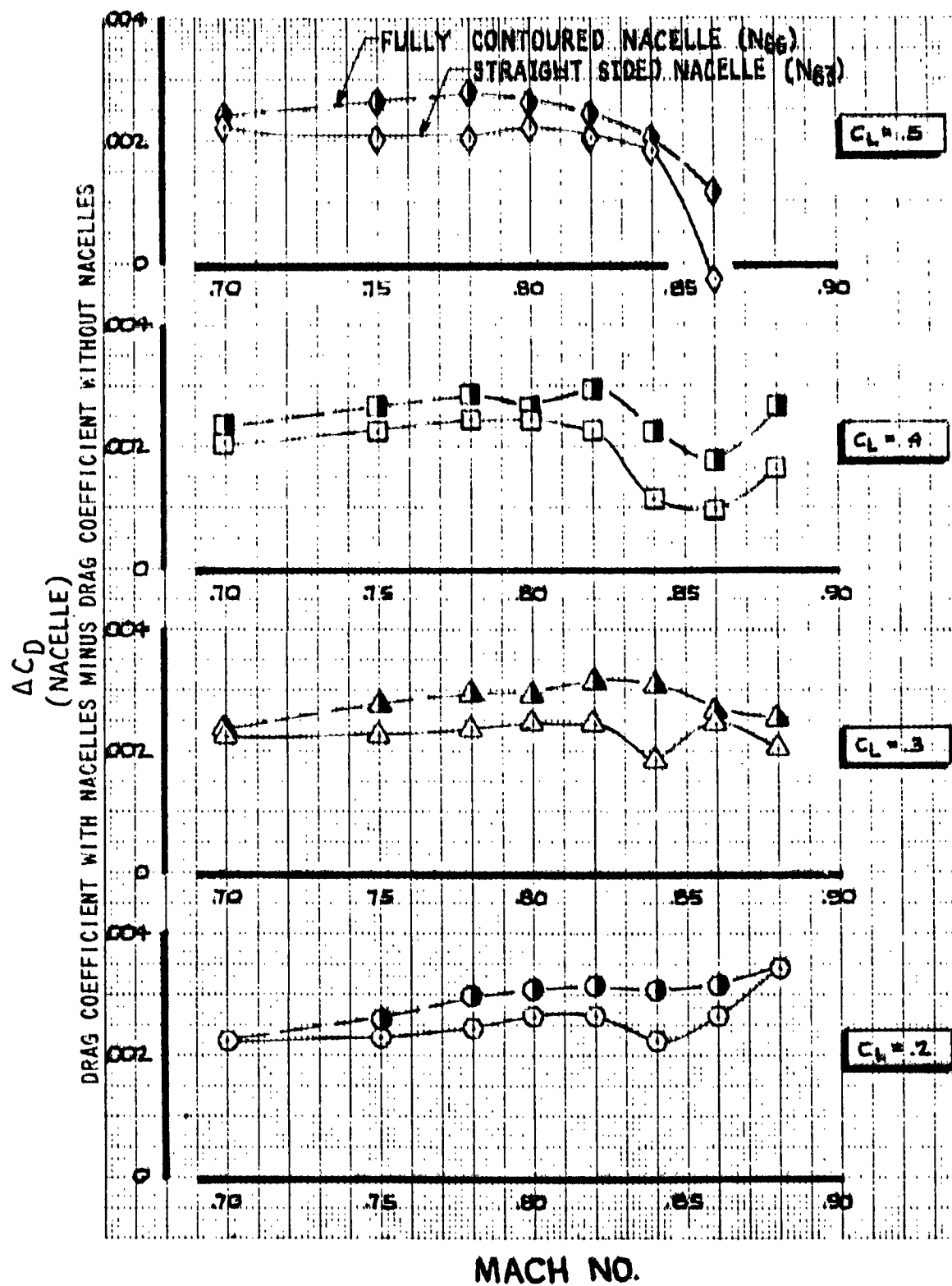


FIGURE 14 DRAG EFFECT OF SIDE NACELLE CONTOUR VARIATION

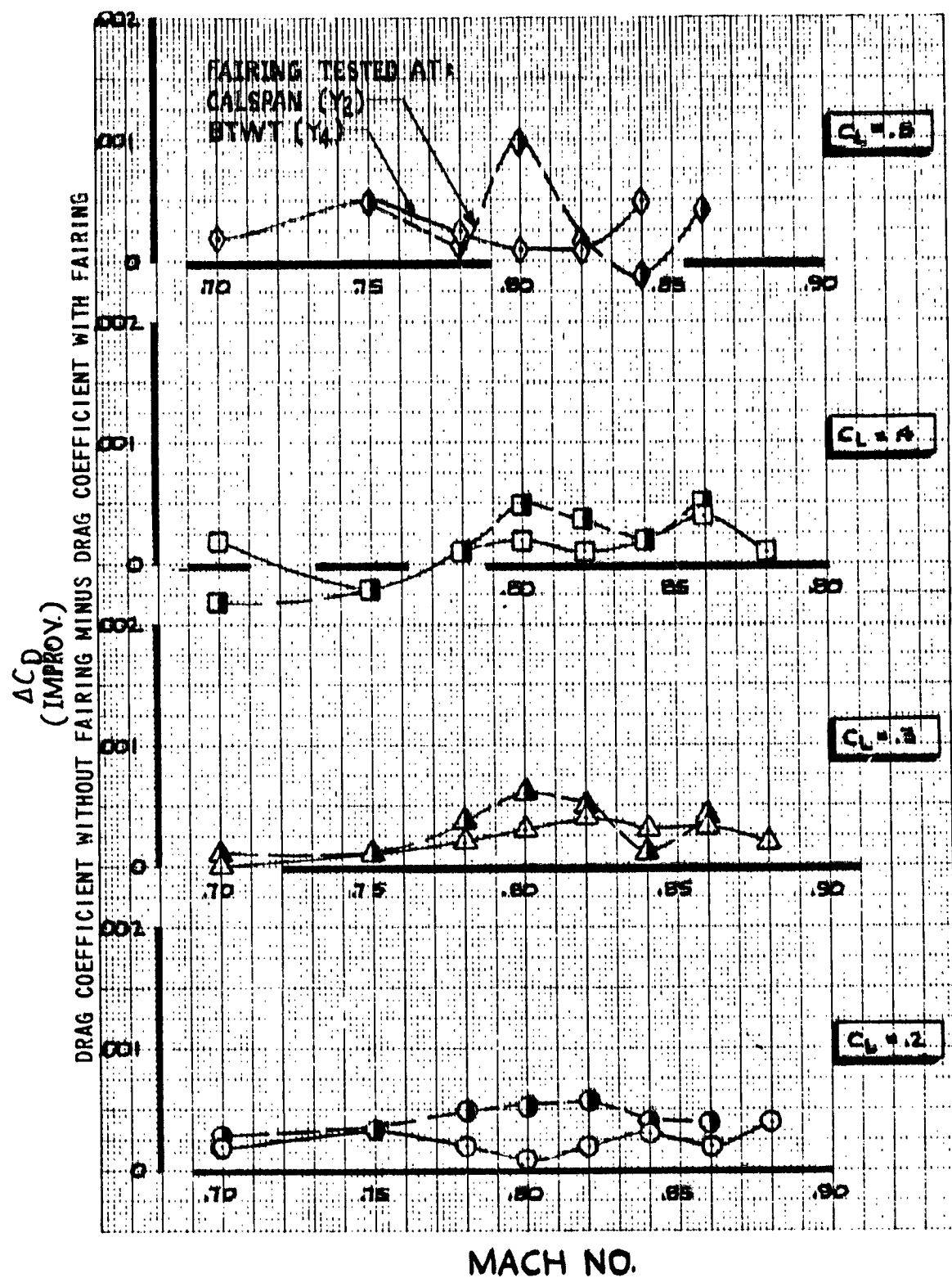


FIGURE 15 DRAG IMPROVEMENT OF STRUT/FUSELAGE FAIRING

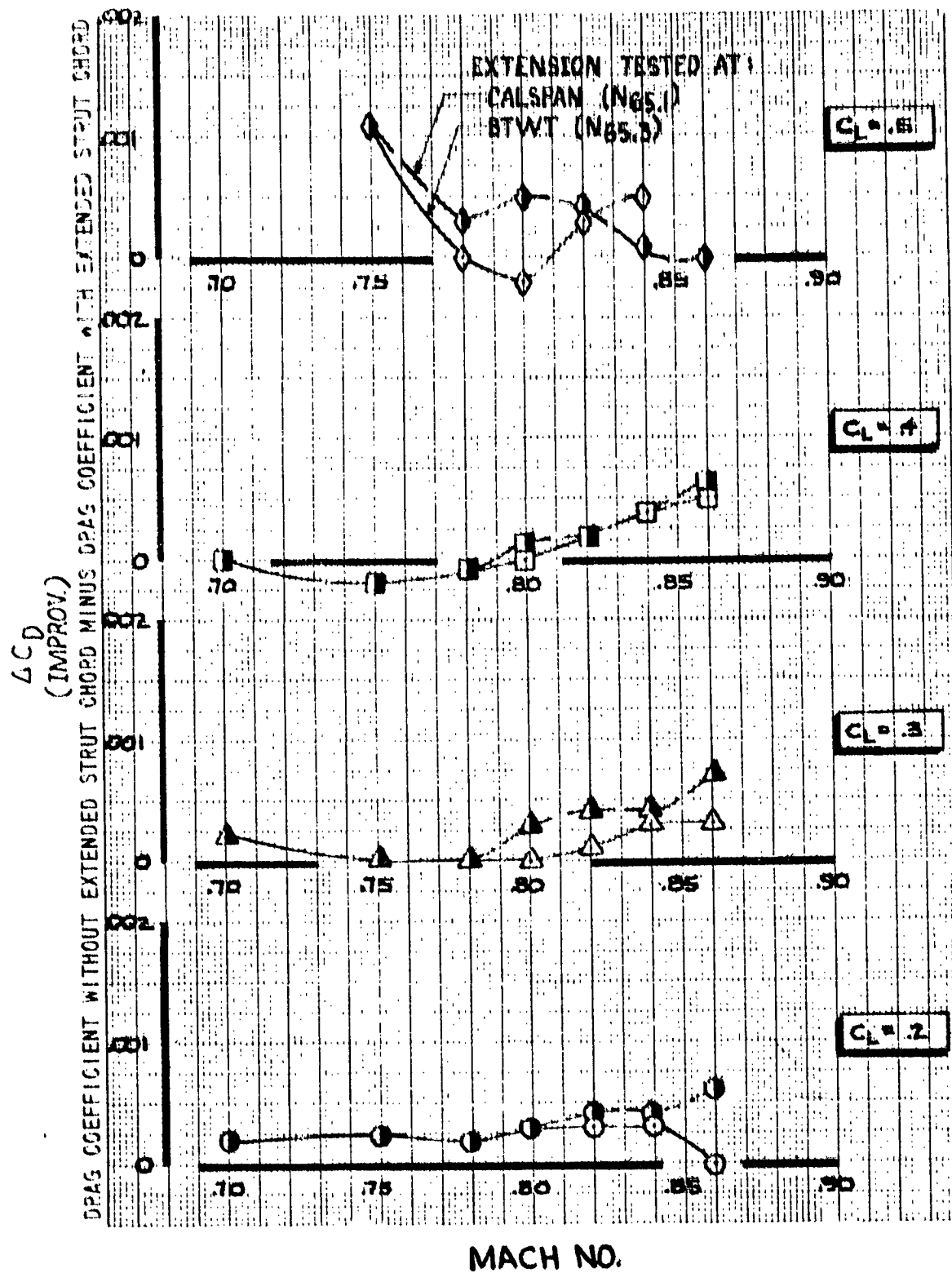


FIGURE 16 DRAG IMPROVEMENT OF STRUT CHORD EXTENSION

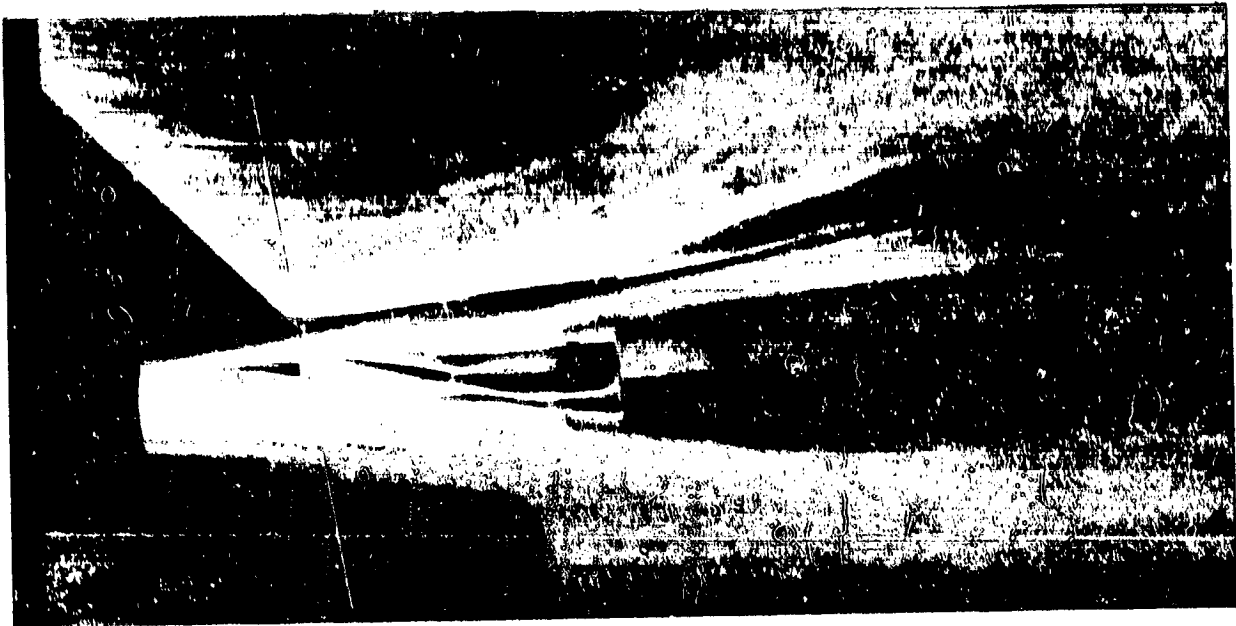


FIGURE 17 OIL FLOW - REFAN STRUT/FUSELAGE FAIRING

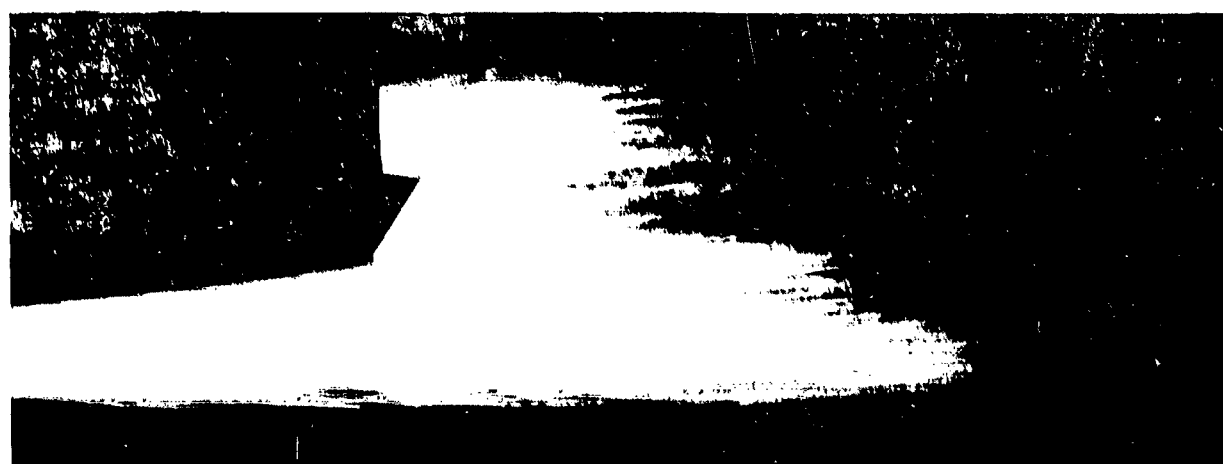
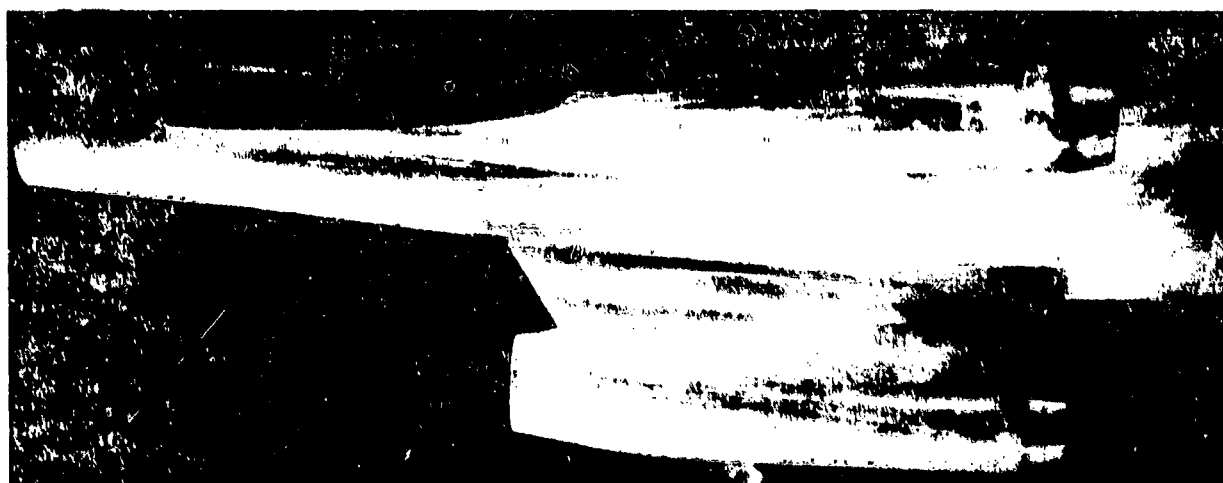


FIGURE 18 OIL FLOW - EXTENDED CHORD STRU1

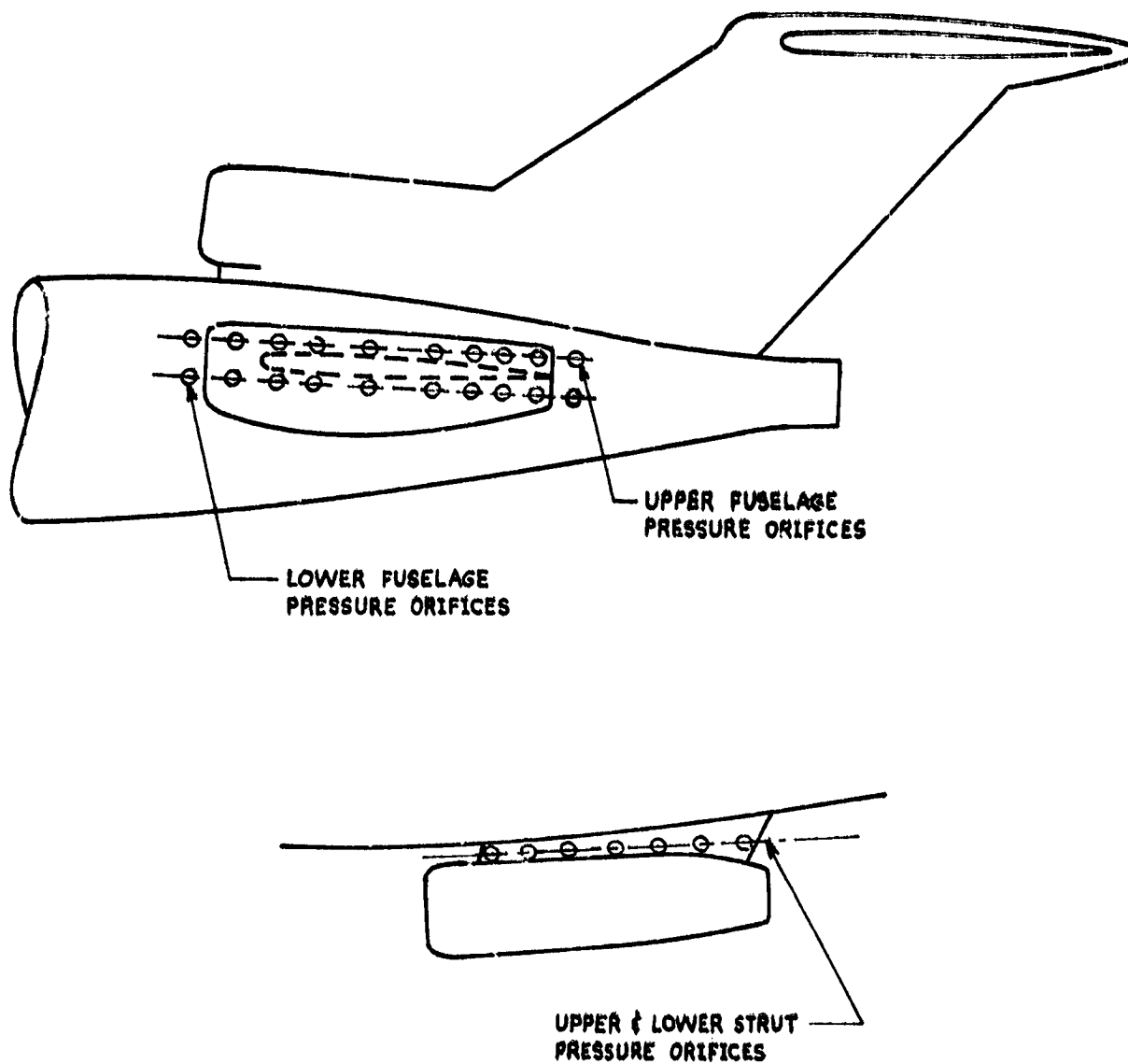


FIGURE 19 SKETCH OF FUSELAGE AND NACELLE STRUT PRESSURE PORT LOCATIONS

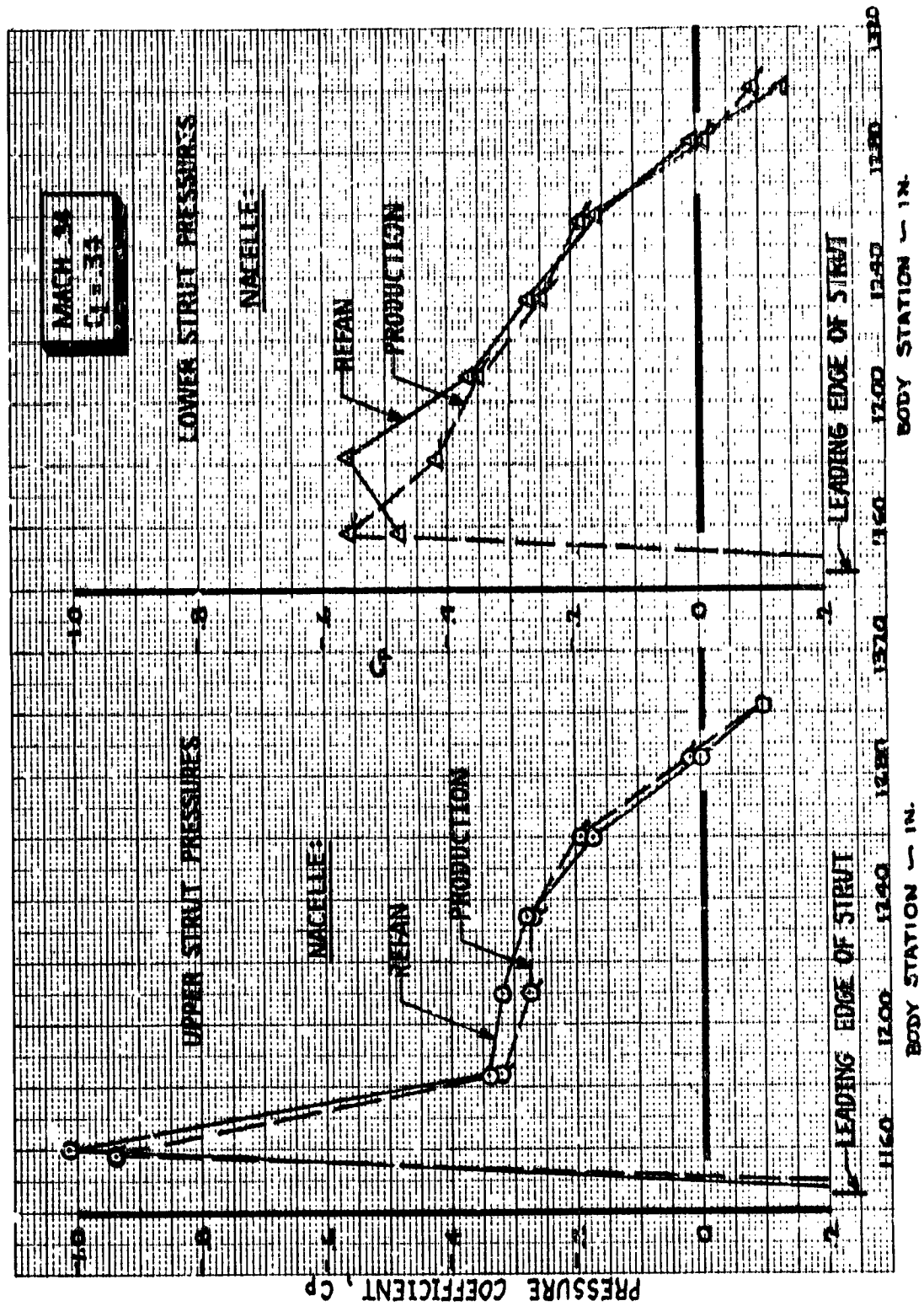


FIGURE 20 COMPARISON OF PRODUCTION AND REAR STATIC PRESSURES

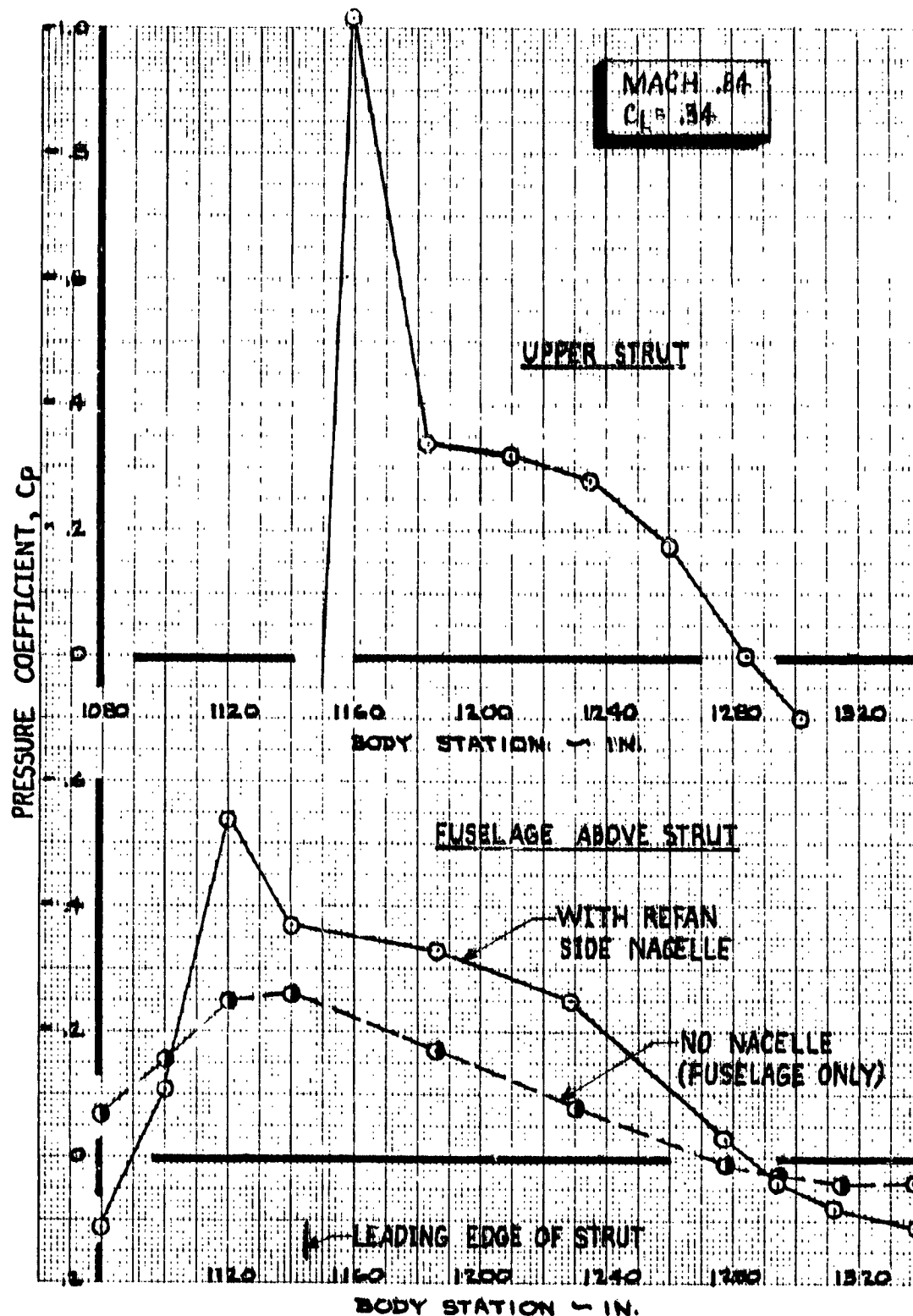


FIGURE 21 STATIC PRESSURES WITH AND WITHOUT REFAN SIDE NACELLE
(UPPER FUSELAGE AND STRUT)

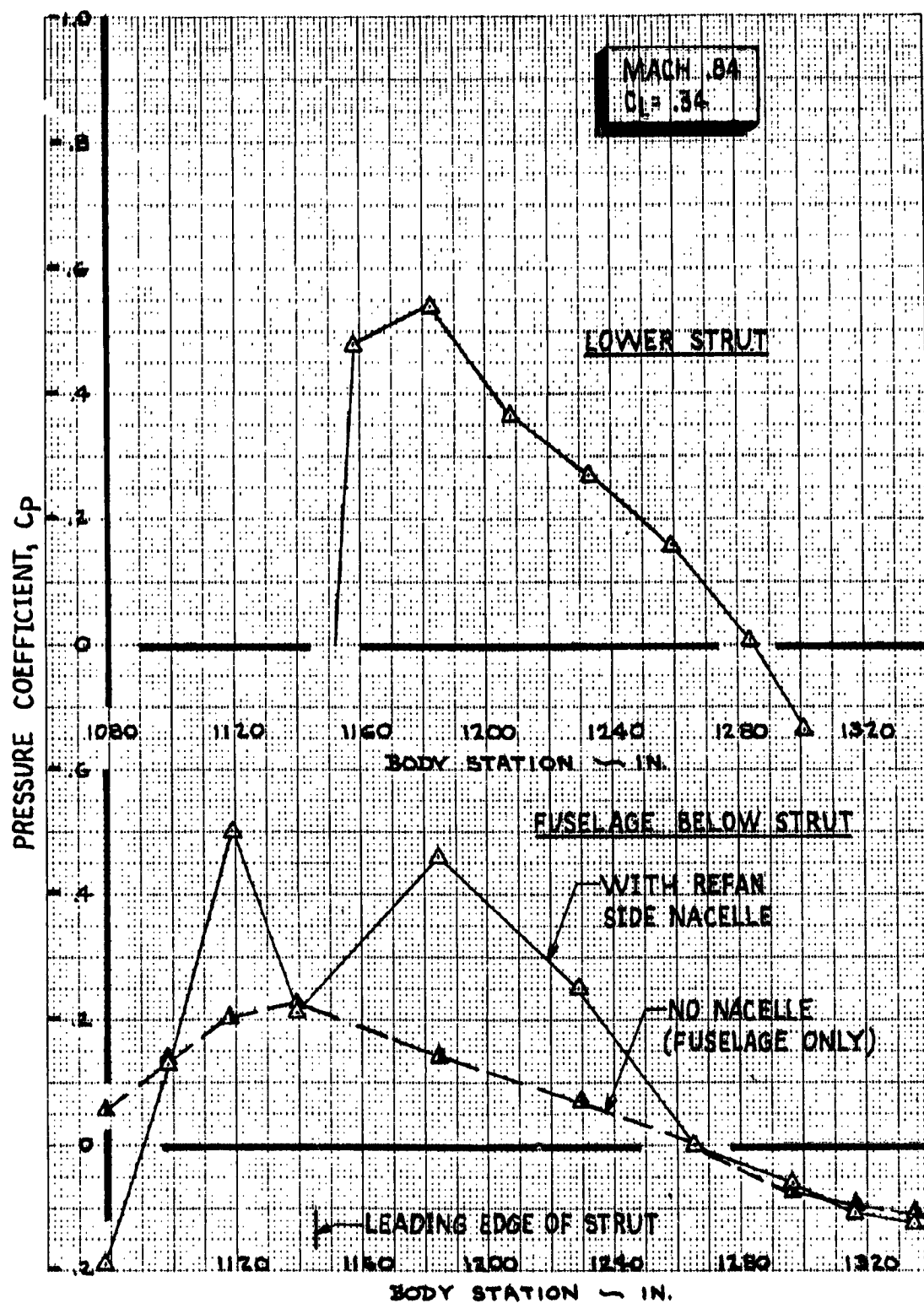


FIGURE 22 STATIC PRESSURES WITH AND WITHOUT REFAN SIDE NACELLE
(LOWER FUSELAGE AND STRUT)

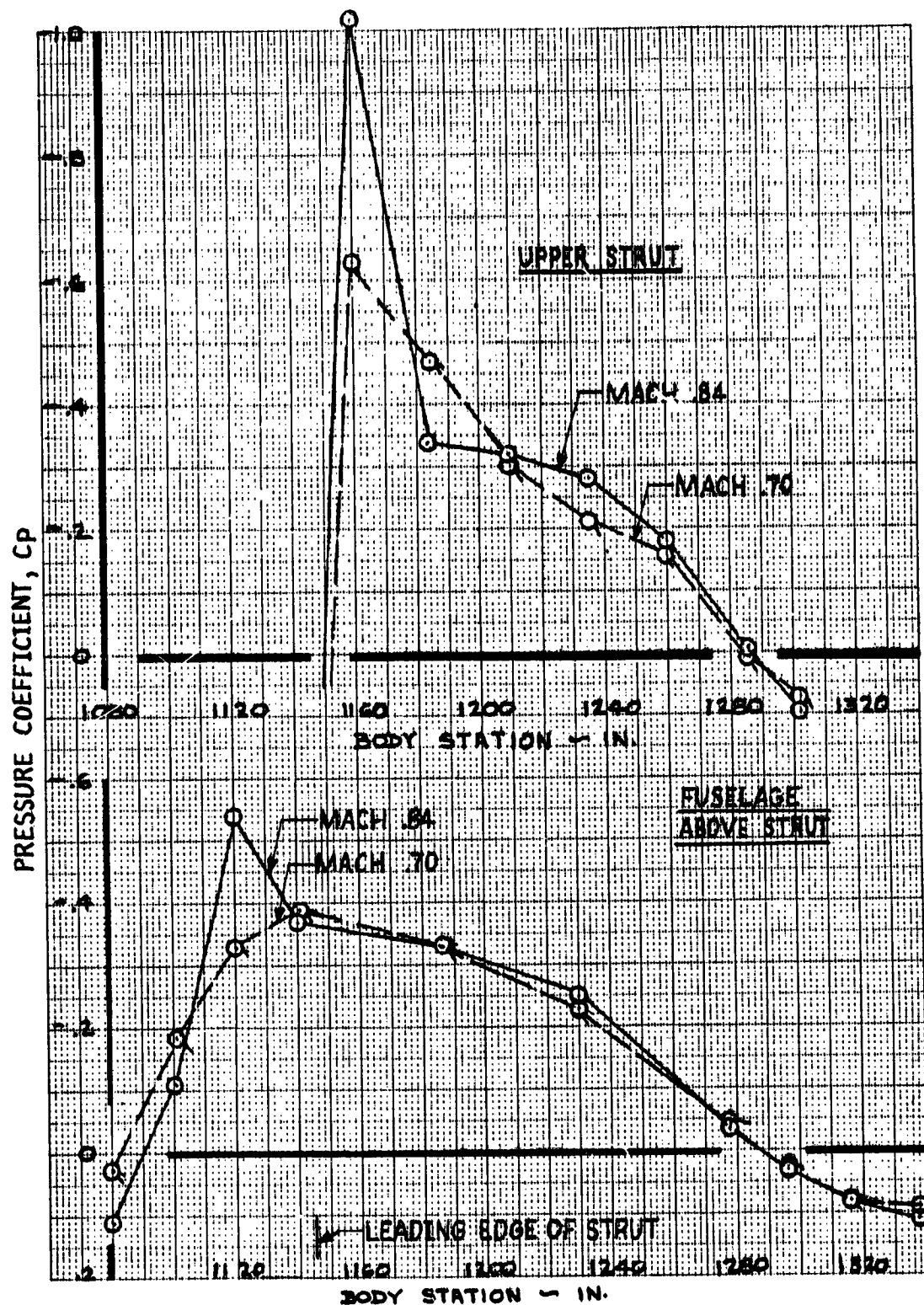


FIGURE 23 EFFECT OF MACH NO. ON REFAN STATIC PRESSURES
(UPPER FUSELAGE AND STRUT)

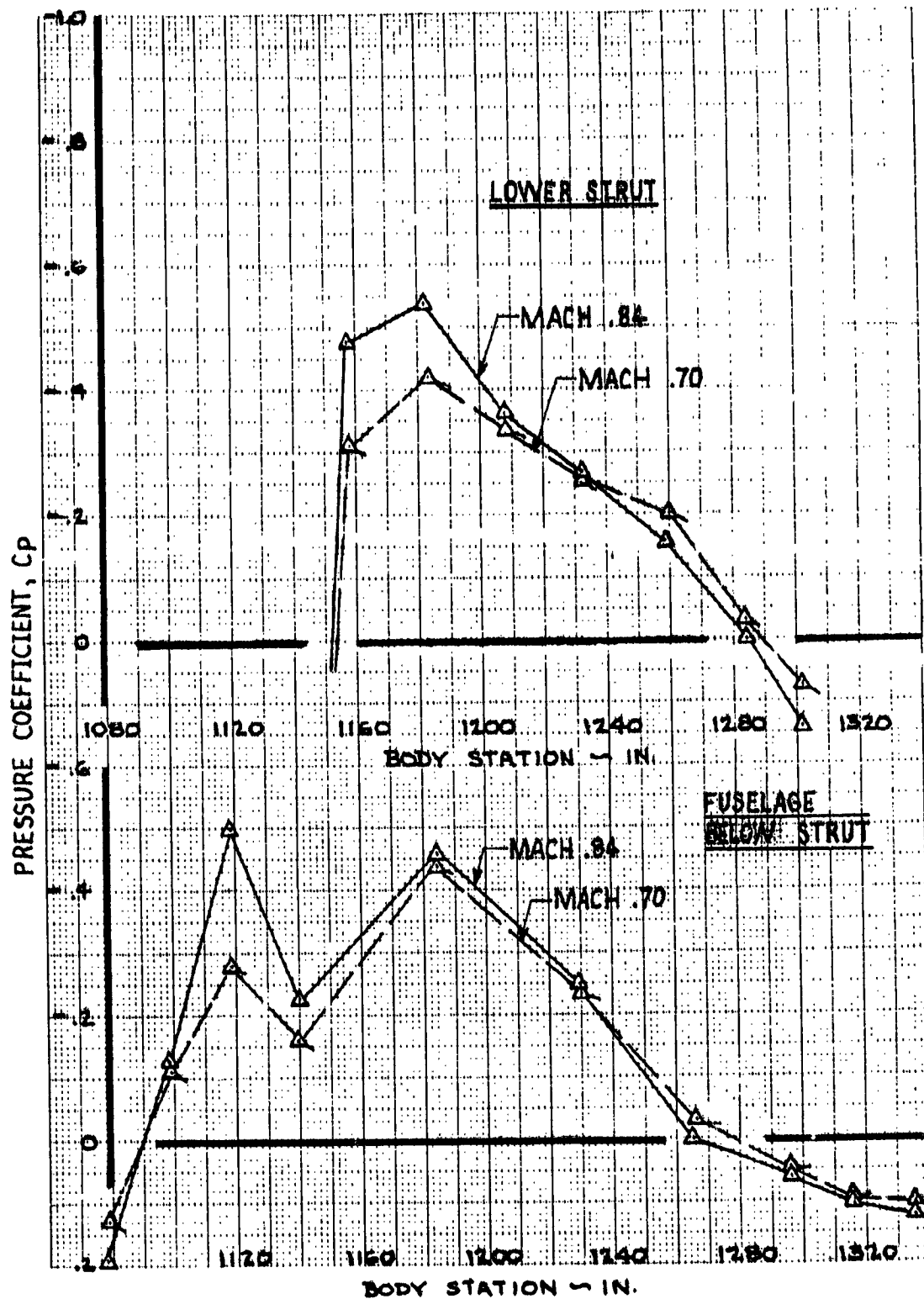


FIGURE 24 EFFECT OF MACH NO. ON REFAN STATIC PRESSURES
(LOWER FUSELAGE AND STRUT)